
Article:
Porter, R.T.J., Mahgerefteh, H., Brown, S. orcid.org/0000-0001-8229-8004 et al. (37 more authors) (2016) Techno-economic assessment of CO2 quality effect on its storage and transport: CO2QUEST. International Journal of Greenhouse Gas Control, 54. P2. pp. 662-681. ISSN 1750-5836

https://doi.org/10.1016/j.ijggc.2016.08.011

Techno-economic Assessment of CO_2 Quality Effect on its Storage and Transport: CO_2QUEST

An overview of Aims, Objectives and Main Findings

Richard T.J. Porter[a,b], Haroun Mahgerefteh[a,*], Solomon Brown[a,†], Sergey Martynov[a], Alexander Collard[a], Robert M. Woolley[b], Michael Fairweather[b], Samuel A.E.G. Falle[c], Christopher J. Wareing[d], Ilias K. Nikolaidis[e], Georgios C. Boulougouris[e], Loukas D. Peristeras[e], Dimitrios M. Tsangaris[e], Ioannis G. Economou[e], Carlos Salvador[f], Kourosh Zanganeh[f], Andrew Wigston[f], John N. Najalafi[f], Ahmed Shafeen[f], Ashkan Beigzadeh[f], Régis Farret[g], Phillipe Gombert[g], Jerome Hebrard[g], Christophe Proust[g], Anthony Ceroni[g], Yann Flauw[g], Yong Chun Zhang[h], Shaoyun Chen[h], Yu Jianliang[h], Reza H. Talemi[i], Jacob Bensabat[j], Jan Lennard Wolf[k], Dorothee Rebscher[k], Auli Niemi[l], Byeongju Jung[l,‡], Niall Mac Dowell[m,n], Nilay Shah[n], Clea Kolster[n], Evgenia Mechleri[n], Sam Krevor[n]

[a]Department of Chemical Engineering, University College London, London WC1E 7JE, UK, [b]School of Chemical and Process Engineering, University of Leeds, Leeds LS2 9JT, UK, [c]School of Mathematics, University of Leeds, Leeds LS2 9JT, UK, [d]School of Physics and Astronomy, University of Leeds, Leeds LS2 9JT, UK, [e]National Center for Scientific Research "Demokritos", Institute of Nanoscience and Nanotechnology, Molecular Thermodynamics and Modelling of Materials Laboratory, Aghia Paraskevi, Attikis GR–153 10, Greece, [f]CanmetENERGY, Natural Resources Canada, Ottowa, K1A 1M1, Canada, [g]INERIS, Parc Technologique ALATA, Verneuil-en-Halatte BP 2, 60550, France, [h]School of Chemical Engineering, Dalian University of Technology, Dalian, People's Republic of China, [i]ArcelorMittal Global R&D Gent-OCAS NV, Pres. J.F. Kennedylaan 3, 9060 Zelzate, Belgium, [j]Environmental and Water Resources Engineering Ltd, Haifa, Israel, [k]Bundesanstalt für Geowissenschaften und Rohstoffe (BGR), Geozentrum Hannover, Stilleweg 2, 30655 Hannover, Germany, [l]Uppsala University, Department of Earth Sciences, Villavägen 16, SE-75236 Uppsala, Sweden, [m]Centre for Environmental Policy, Imperial College London, London SW7 1NA, UK, [n]Centre for Process Systems Engineering, Department of Chemical Engineering, Imperial College London, London SW7 2AZ, UK.

[†]Current address: Department of Chemical and Biological Engineering, University of Sheffield, Sheffield, London S1 3JD, UK.

[‡]Current address: Division of Earth Environment Research, Korea Institute of Geoscience and Mineral Resources, Daejeon 305-350, South Korea.

[*]Corresponding author and CO_2QUEST Project Coordinator: Tel: +44(0)207 679 3835

Email address: H.Mahgerefteh@ucl.ac.uk (Haroun Mahgerefteh).

Submission of a full-length article to the International Journal of Greenhouse Gas Control, of unpublished material not submitted for publication elsewhere

ABSTRACT

This paper provides an overview of the aims, objectives and the main findings of the CO_2QUEST FP7 collaborative project, funded by the European Commission designed to address the fundamentally important and urgent issues regarding the impact of the typical impurities in CO_2 streams captured from fossil fuel power plants and other CO_2 intensive industries on its safe and economic pipeline transportation and storage. The main features and results recorded from some of the unique test facilities constructed as part of the project are presented. These include an extensively instrumented realistic-scale test pipeline for conducting pipeline rupture and dispersion tests in China, an injection test facility in France to study the mobility of trace metallic elements contained in a CO_2 stream following injection near a shallow-water qualifier and fluid/rock interactions and well integrity experiments conducted using a fully instrumented deep-well CO_2/impurities injection test facility in Israel. The above, along with the various unique mathematical models developed, provide the fundamentally important tools needed to define impurity tolerance levels, mixing protocols and control measures for pipeline networks and storage infrastructure, thus contributing to the development of relevant standards for the safe design and economic operation of CCS.

Dedication: This paper is dedicated to the memory of our friend and colleague, Dr. Robert M. Woolley, who made a significant input to the CO_2QUEST project and whose expertise, commitment and support inspired many of those around him.

KEYWORDS

CCS, CCS cost/benefit analysis, CCS safety, CO_2 impurities, multi-phase flow, mathematical modelling.

1. INTRODUCTION

For large-scale applications of CO_2 Capture and Storage (CCS), transport of CO_2 using high pressure pipelines is found to be the most practical and economic method (Serpa et al., 2011). However the CO_2 stream captured from fossil fuel power plants or other CO_2 intensive industries will contain a range of different types of impurities each having its own impact on the different parts of the CCS chain. Such impurities may be classified broadly by origin into three main categories arising from fuel oxidation, excess oxidant/air ingress, and process fluids as shown in Table 1 (Porter et al., 2015). Water is a major combustion product and is considered an impurity in the CO_2 stream. The elements inherently present in a fuel such as coal include sulfur, chlorine and mercury, and are released upon complete or incomplete combustion and form compounds in the gas phase which may remain to some extent as impurities in the CO_2 after it is captured and compressed. The oxidising agent used for combustion, such as air, may result in residual impurities of N_2, O_2 and Ar; these same impurities may also result from any air ingress into the process. The materials and chemicals used for the CO_2 separation process, such as monoethanolamine (MEA) used for post-combustion capture, or Selexol in pre-combustion capture, and their degradation products can be carried over into the CO_2 stream constituting a further class of impurity.

Table 1. Classes of potential CO_2 impurities by origin.

Coal/biomass oxidation products	
Complete	Partial
H_2O, SO_X, NO_X, HCl, HF	CO, H_2S, COS, NH_3, HCN
Volatiles	Biomass alkali metals
H_2, CH_4, C_2H_6, C_3+	KCl, NaCl, K_2SO_4, KOH etc.
Trace metals	Particulates
Hg ($HgCl_2$), Pb, Se, As etc.	Ash, PAH/soot
Oxidant / air ingress	**Process fluids**
O_2, N_2, Ar	Glycol, MEA, Selexol, NH_3 etc.

Impurities that arise from CO_2 capture sources can have a number of important impacts on the downstream transport and storage infrastructure and operation. The presence of impurities in CO_2, such as air derived non-condensable species (N_2, O_2 and Ar), can shift the dew point and bubble point lines on the mixture phase diagram to higher pressures compared with pure CO_2. As a result higher operating pressures will be needed to keep CO_2 in the dense phase, thus impacting on compression and transport costs. In addition, these species can reduce the

CO_2 structural trapping capacity in geological formations by a greater degree than their molar fractions (Wang et al., 2012). Hydrogen may be present in pre-combustion capture derived CO_2 streams, introducing the risk of embrittlement of the pipeline steel. Additionally, hydrogen significantly affects the rate of inventory pressure loss during pipeline transportation of CO_2 (Wetenhall et al., 2014). Enhanced Oil Recovery applications require stricter limits, particularly on O_2 due to its promotion of microbial growth and reaction with hydrocarbons. Water should be limited in CCS applications in order to avoid corrosion arising from the formation of in situ carbonic acid (Cole et al., 2011) along with clathrate formation and condensation (Serpa et al., 2011). Conversely, water may be of benefit even at high concentrations in storage given its immobilisation effect on CO_2.

Sulfur species (H_2S, COS, SO_2 and SO_3) may pose a corrosion risk in the presence of water and there are additional toxicity concerns for H_2S. NO_X species may be present in CO_2 streams as combustion by-products, posing a corrosion risk due to nitric acid formation (Sim et al., 2013). Trace elements such as Lead, Mercury and Arsenic in the CO_2 stream are of concern for geological storage due to their toxicity and the possibility that they could contaminate groundwater. Amongst the numerous potential trace metal CO_2 impurities, mercury receives further attention for its corrosive effects on a number of metals. Due to its toxicity, limits are also suggested for carbon monoxide. For other components that may be present in CO_2 streams (e.g., HCl, HF, NH_3, MEA, Selexol), not enough information is available to fully understand their downstream impacts on transport and storage and thus determine maximum allowable amounts. Further work is therefore required to understand the impacts of these species in transport and storage applications and to elucidate potential crossover effects.

In CCS systems, capture costs can be expected to increase with increasing CO_2 purity as additional process unit operations and the increased energy penalty associated with achieving purer CO_2 is taken into consideration. Conversely, transport and storage costs (per tonne of CO_2 transported) may be expected to decrease with increasing CO_2 purity due to the lower compression requirements to keep CO_2 in the dense phase, lower rates of corrosion and the relaxation of safety measures needed to deal with hazardous impurities. When capital and operating costs are factored together to calculate a levelised “total cost” for CCS systems a minima for a given purity and composition range is expected where the system may be assumed to be cost optimised in addition to having the necessary safety precautions

implemented. The challenge therefore is to find the optimum range and concentration of impurities that can be permitted in a CO_2 stream to enable its safe and cost-effective transportation and storage.

The CO_2QUEST project addresses the fundamentally important issues surrounding the impact of the typical impurities in CO_2 streams derived from fossil fuel power plants or other CO_2 intensive industry on the safe and economic transportation and storage of CO_2. Based a techno-economic analysis, CO_2QUEST elucidates the optimum level of CO_2 purification required for CCS in consideration of the effects of impurities on pipeline transportation, geological storage and the purification costs with safety and environmental issues being the overarching factors.

This paper describes the objectives, methodology and the main findings of the CO_2QUEST project. Section 2 defines the project's scope and work package structure. Section 3 discusses the fluid properties and phase behaviour of CO_2 mixtures, characterising the CO_2 stream impurities and determining their physical properties. Sections 4 and 5 cover the impact of CO_2 stream impurities on pipeline transportation, compression and storage. The techno-economic methodology and risk assessment work is presented in Section 6, followed by Conclusions in Section 7.

2. PROJECT WORKPACKAGES

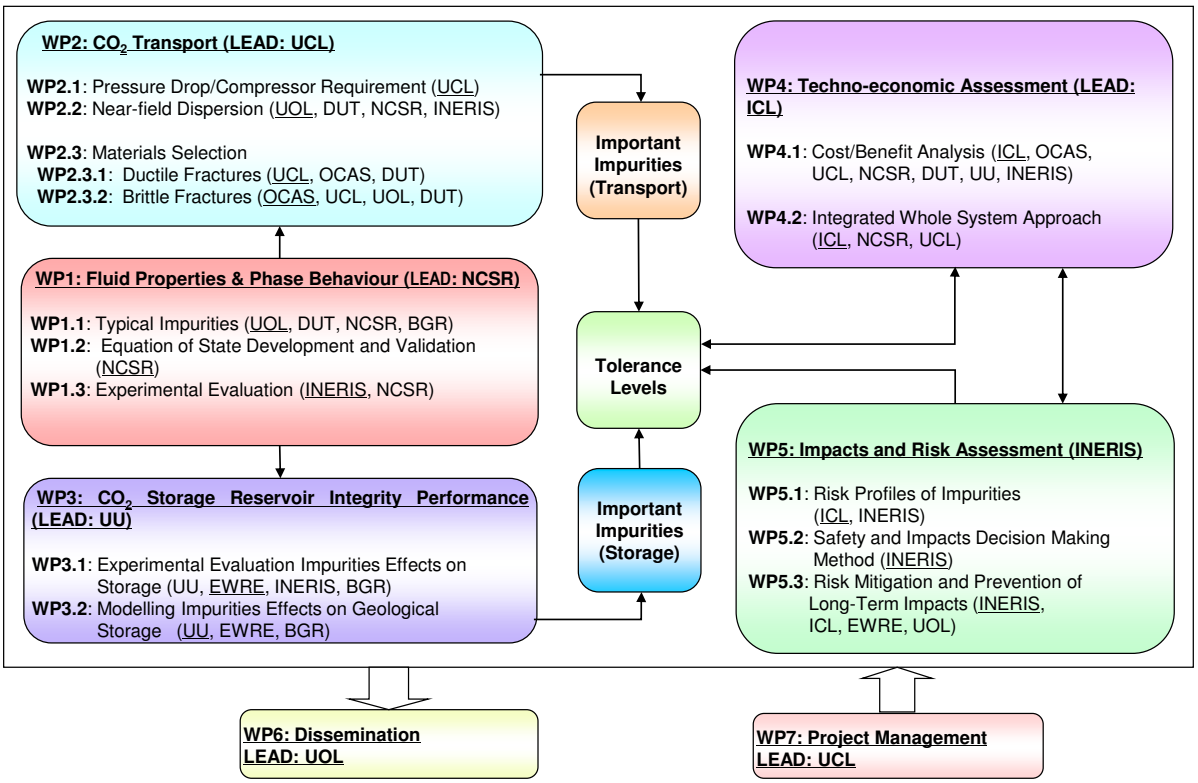

Figure 1. Pert diagram representation of the CO_2QUEST project structure.

Figure 1 presents the CO_2QUEST project structure in the form of various Work Packages (WPs) along with their interactions. The following sections provide summary descriptions of the aims, objectives and main findings of each WP.

3. WP1 – FLUID PROPERTIES AND PHASE BEHAVIOUR

3.1 Typical impurities and cost-benefit analysis

The work in this section, based on literature studies, underpins the other project activities by providing analysis of the ranges and levels of impurities present in CO_2 streams derived from different carbon capture sources, including those from both the power sector and heavy industries. The factors that affect the ranges and levels of impurities for given power generation technologies, such as post-combustion, pre-combustion and oxyfuel combustion capture, have also been identified leading to the ranges as set out in Table 2.

Table 2. CO_2 impurities from different CO_2 capture technologies

	Oxyfuel Combustion			Pre-combustion	Post-combustion
	Raw / dehumidified	Double flashing	Distillation		
CO_2 % v/v	74.8-85.0	95.84-96.7	99.3-99.9	95-99	99.6 – 99.8
O_2 % v/v	3.21-6.0	1.05-1.2	0.0003-0.4	0	0.015 – 0.0035
N_2 % v/v	5.80-16.6	1.6-2.03	0.01-0.2	0.0195 – 1	0.045 - 0.29
Ar % v/v	2.3-4.47	0.4-0.61	0.01-0.1	0.0001-0.15	0.0011 – 0.021
NO_x ppmv	100-709	0-150	3-100	400	20 - 38.8
SO_2 ppmv	50-800	0-4500	1-50	25	0 - 67.1
SO_3 ppmv	20	-	0.1-20	-	N.I.
H_2O ppmv	100-1000	0	0-100	0.1 - 600	100 – 640
CO ppmv	50	-	2-50	0 - 2000	1.2 - 10
H_2S/COS ppmv				0.2 - 34000	
H_2 ppmv				20-30000	
CH_4 ppmv				0-112	

A techno-economic modelling study of power plants with CO_2 capture technologies which focusses on process scenarios that deliver different degrees of CO_2 stream purity was also carried out in this work package. The three leading CO_2 capture technologies for the power sector are considered, namely; oxyfuel combustion, pre-combustion and post-combustion capture. The study uses a combination of process simulation of flue gas cleaning processes, modelling with a power plant cost and performance calculator and literature values of key performance criteria in order to calculate capital costs, operational and maintenance costs, the levelised cost of electricity and CO_2 product purity of the considered CO_2 capture options (Porter et al., in prep).

For oxyfuel combustion capture, the calculations are based on a 400 MWg retrofitted power station that uses a low sulfur coal and considers three raw CO_2 flue gas processing strategies of compression and dehydration only, double flash system purification and distillation

purification. Analysis of pre-combustion capture options is based on new build integrated gasification combined cycle plants with one gas-turbine and a GE entrained-flow gasifier. Integrated physical solvent systems for capturing CO_2 and sulfur species were considered in three ways; co-capture of sulfur impurities with the CO_2 stream using Selexol^{TM} solvent or separate capture of CO_2 and sulfur impurities using either Selexol^{TM} or Rectisol$^{®}$ solvent systems. Analysis of post-combustion capture plants was made with and without some conventional pollution control devices.

Of the different cases considered, pre-combustion capture with co-capture of impurities and CO_2 using Selexol^{TM} offered the lowest cost with a reasonably high purity of CO_2 at 97.64 mol%, but high estimated levels of H_2S (at 3974 ppm_v) in the captured stream. The most expensive system was pre-combustion capture using Rectisol$^{®}$ with separate capture of CO_2 and sulfur impurities, producing a dry 99.51 mol% pure CO_2 stream. The system with the lowest grade of CO_2 was oxyfuel combustion capture with compression and dehydration of the raw CO_2 stream only, which resulted in 77.69 mol% pure CO_2 and with the second lowest cost. The oxyfuel plant with a distillation purification system and a post-combustion capture plant with conventional pollution control devices had the joint highest CO_2 purity (99.99 mol%), with the post-combustion capture system estimated to be the cheaper of the two. The calculations performed are of use in further analyses of whole chain CCS for the safe and economic capture, transport and storage of CO_2.

3.2 Equation-of-state development for CO_2 mixtures and supporting vapour liquid equilibrium data

The Vapour – Liquid Equilibrium (VLE) of CO_2 mixtures associated with CCS processes has attracted significant attention both in terms of experimental measurements and modelling using macroscopic models such as equations of state (EoS). Nevertheless, a critical part of the design and operation of CCS facilities is the study of solidification phenomena when CO_2 mixes with other gases. Relatively little work has been performed to measure and predict the solid-fluid equilibrium (SFE) of these mixtures. CO_2 possesses a relatively high Joule–Thomson coefficient, as a result during transport a sudden pipeline depressurization will lead in rapid cooling and potentially very low fluid temperatures (Woolley et al., 2014). Consequently, solid formation may occur. The objective of this work is the application of

solid thermodynamic models of different complexity to model the SFE of pure CO_2 and of CO_2 mixtures with other compounds, including N_2, H_2 and CH_4.

Three solid thermodynamic models have been coupled with vapour-liquid EoS to model the SFE of pure CO_2 and binary mixtures of CO_2 with other gases associated with CCS processes. The solid models include an empirical correlation fitted to experimental data at SFE conditions, a model based on thermodynamic integration and an EoS developed for pure, solid CO_2. The solid models have been coupled with Peng-Robinson (PR), Soave-Redlich-Kwong (SRK) and Perturbed Chain-Statistical Associating Fluid Theory (PC-SAFT) EoS which are used widely for liquids and gases. Firstly, every model was evaluated to correlate the pure CO_2 solid-liquid (SLE) and solid-vapour (SVE) equilibrium. This way the performance of a solid model coupled with different EoS is tested and the agreement between the different models is assessed. Moreover, an accurate description of the SFE behaviour of pure CO_2 is a good basis for subsequent two phase and three phase solid-liquid-gas equilibrium (SLGE) mixture calculations. Because of lack of experimental data for two phase SFE for the CO_2 mixtures of interest, the performance of the different models has been evaluated on SLGE conditions, and compared to experimental data from literature (Fandiño et al., 2015; Davis et al., 1962).

The modelling results have shown that a model that successfully reproduces the pure CO_2 triple point will more accurately predict the SLG locus of the mixture. In this context, the thermodynamic integration model and the Jäger and Span (2012) EoS provide, in general, more accurate predictions of the SLGE for the mixtures of CO_2 with N_2 and $H_2$when all binary interaction parameters (BIPs) are zero. For these two mixtures, the empirical correlation model for the solid phase is comparable to the other two models only when coupled with PC-SAFT, which accurately reproduces the pure CO_2 triple point. The use of BIPs, regressed from binary VLE data at low temperature, significantly improves the prediction of the SLG behaviour for most models. All models provide very similar results for the CO_2 – CH_4 mixture and very low deviations from experimental data have been achieved with the use of BIPs regressed from binary VLE data over a wide temperature range. A representative example is shown in Figure 3 for the three CO_2 mixtures and refers to calculations with the thermodynamic integration model coupled with the PC-SAFT EoS.

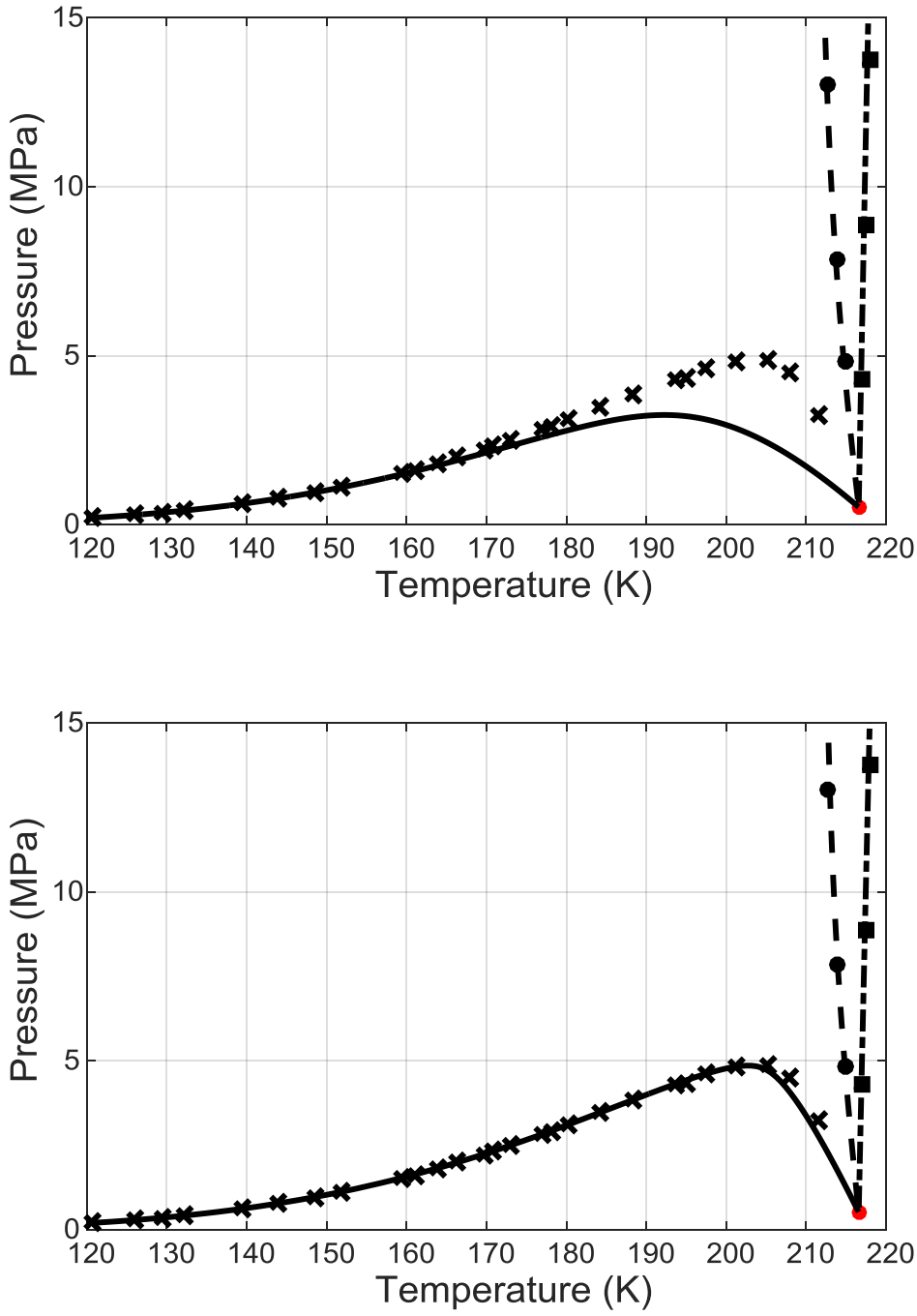

Figure 3. Calculation of the SLG equilibrium curves of binary CO_2 mixtures with the Thermodynamic Integration model, coupled with PC-SAFT EoS. Experimental data are represented by points for the following mixtures: (●) CO_2 – N_2, (■) CO_2 – H_2 and (**x**) CO_2 – CH_4. Calculations are shown with lines: (– – –) CO_2 – N_2, (– · –) CO_2 – H_2 and (–) CO_2 – CH_4. Top panel shows predictions ($\mathbf{k_{ij} = 0}$), while bottom panel shows calculations when temperature-independent $\mathbf{k_{ij}}$ parameters fitted to experimental binary VLE data are used.

3.3 Acquisition of Vapour Liquid Equilibrium Data for CO_2 Mixtures

Accurate knowledge of the thermodynamic properties of CO_2 mixtures is essential in the design and operation of CCS systems. The Vapour-Liquid-Equilibrium (VLE) of CO_2 mixtures is, for example, one of the basic parameters required to design a CO_2 capture process as well as non-condensable gas separation processes. Available experimental data and the theoretical models associated with the thermodynamic properties of CO_2 mixtures within the operation window of CCS are scarce (Ahmed et al., 2014). This is particularly the case for multi-component CO_2 mixtures. However, it should be noted that CCS processes cover a large range of operation conditions from atmospheric pressure to supercritical states, therefore experiments alone cannot satisfy the requirements of engineering applications (Chapoy et al., 2013). In order to exceed the limitations of the available experiments theoretical models in the form of EoS need to be developed using experimental data. However, many EoS available in the literature do not show any clear advantage in CCS applications for the calculation of properties of multi-component CO_2 mixtures. Hence, the objective of this work is to conduct experiments with CO_2 mixtures relevant to the CCS chain to obtain experimental data that can be used to develop reference equations of state for CCS applications.

CanmetENERGY is providing experimental VLE data for multi-component CO_2 mixtures to support our efforts to develop EoS relevant to CCS systems. In this context, CanmetENERGY has built a CO_2 pressure cell test facility capable of reaching and maintaining a two-phase equilibrium for multi-component CO_2 mixtures while separately measuring the composition and density of both liquid and vapour phases (Figure 4). Under this collaborative effort, experimental VLE composition and density data is acquired for three different CO_2 mixtures; namely CO_2-O_2-N_2-Ar, CO_2-SO_2-N_2, and CO_2-CH_4-N_2. This data is acquired in the ranges 300 to 220 K at increments of 20 K and 5 to 80 bar at increments of 5 bar. Experiments are performed in a thermally stable environment where the temperature is controlled to 0.01 K. In addition to tight temperature control, equilibrium of the two-phase mixtures is maintained by a pump that continually mixes the two-phase mixture to ensure that equilibrium is achieved and maintained throughout the experiments.

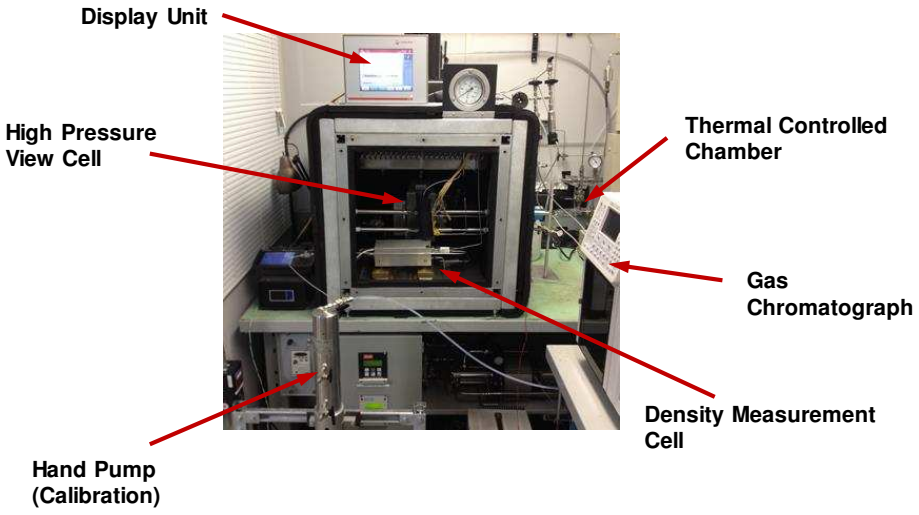

(a)

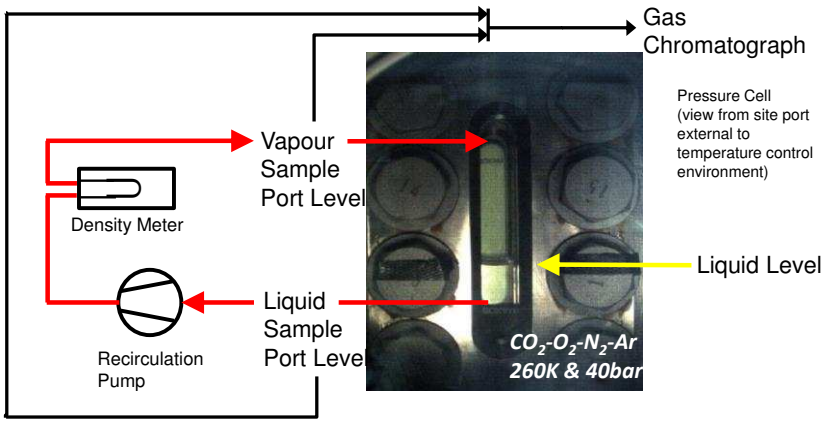

(b)

Figure 3. CanmetENERGY's CO_2 Pressure Cell Test Facility (a); and, sampling arrangement (b).

Main Research Outcomes

At the outset experiments were conducted with pure CO_2 to set the baseline and verify the methodology, calibration procedures, accuracy and consistency of the measuring devices. Data from the National Institute of Standards and Technology (NIST) (Chickos, 2005) was used as a control dataset. Subsequently tests were conducted with the selected quaternary CO_2 mixtures discussed above. The experimental data were compared with pure CO_2 measurement results, similarities in the general trends in the vapour phase were observed but more pronounced differences existed in the liquid phase. Further, quaternary CO_2 gas mixtures were prepared and tested within the targeted ranges of pressure and temperature,

VLE composition and density data was acquired and compared to HYSYS simulation results using the Peng–Robinson EoS (HYSYS, 2014; Peng and Robinson, 1970). There were some deviations from predicted HYSYS results at high pressures, particularly in the vapour phase, as depicted in Figure 5; however the overall trends showed reasonable agreement. The experimental data was shared with NCSR to further adjust and verify their equation of state. The outcome of the latter activity has been presented in the previous section.

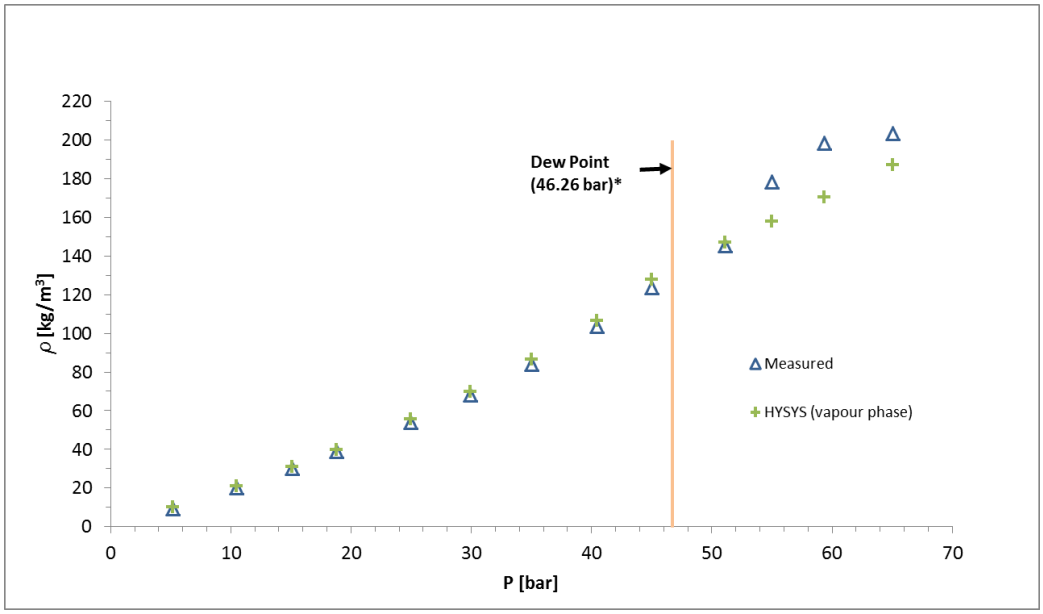

Figure 5. Vapour phase density measurement HYSYS (Peng-Robinson EOS) Calculated Value vs. Measure CO_2-O_2-N_2-Ar as Mixture (93%-5.41%-1.49%-649 ppm), T = 280K.

The experimental work conducted by CanmetENERGY led to a unique database for the properties of CO_2 mixtures that are relevant to CCS systems. Moreover, this experimental campaign provided the research team at CanmetENERGY with the opportunity to optimize and fine-tune their experimental apparatus, calibration, sampling and test procedures. In this respect extensive and unique operational experience was gained. This capacity can be made available to other research initiatives in order to support future EoS development or other research efforts.

4. WP2 – CO_2 Transport

4.1 Pressure drop and compressor requirement

In this section we present the modelling of non-isothermal steady-state flow carried out in order to calculate pressure drop (and hence compressor power requirements) in pipeline networks transporting CO_2 with typical stream impurities using the dedicated EoS developed under WP1 (see figure 1 and Section 3.2). Compression strategies for minimising compressor power requirements have been developed. We have also performed parametric studies using a developed flow model to identify the type and composition of stream impurities that have the most adverse impact on the CO_2 pipeline pressure drop, pipeline capacity, fluid phase and compressor power requirements.

Compressor Power Requirements

Minimising the pressure drop and avoiding two-phase flows within CO_2 pipeline networks is essential for reducing compressor power requirements. This is critically important given that the compression penalty for CO_2 capture from coal-fired power plants is estimated to be as high as 12% (Moore et al., 2011). In order to evaluate the impact of CO_2 impurities on compressor power requirements a thermodynamic analysis method is applied to CO_2 streams captured using oxy-fuel, pre-combustion and post-combustion capture technologies, stream compositions were derived from Table 2. The analysis is performed for several methods of compression previously recommended for pure CO_2, including the following options (Witkowski and Majkut, 2012):

- Option A: Centrifugal integrally – geared multistage compressors.
- Option B: Supersonic axial compressors.
- Option C: Compressors combined with liquefaction followed by pumping.

Figure 5 shows an example of the calculation of thermodynamic paths for multi-stage compression combined with intercooling relative to the phase envelopes for pure and impure CO_2 streams. Figure 6 shows the power consumption for each compression strategy (options A, B and C) for mixtures representing all capture technologies.

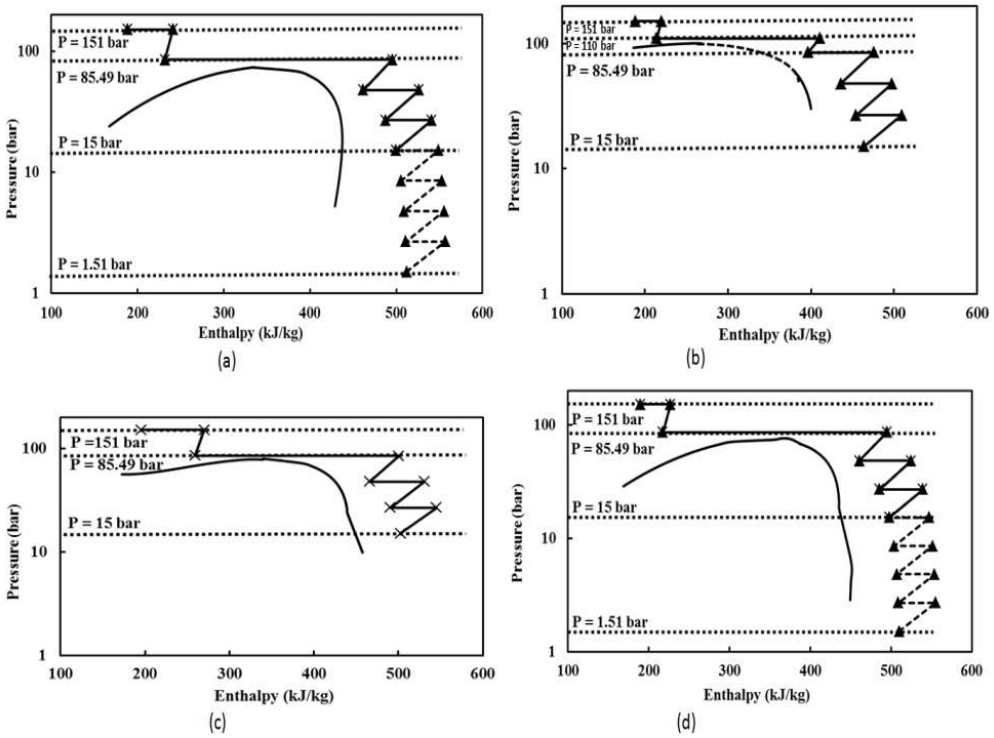

Figure 5. The thermodynamic paths for compression of pure CO_2 (a) and CO_2 mixtures from oxy-fuel (b), pre-combustion (c), and post-combustion (d) capture using compression and pumping with supercritical liquefaction. Note that the compressor inlet pressure is 1.5 bar for pure CO_2 and post-combustion streams and 15 bar for the pre-combustion and oxy-fuel streams.

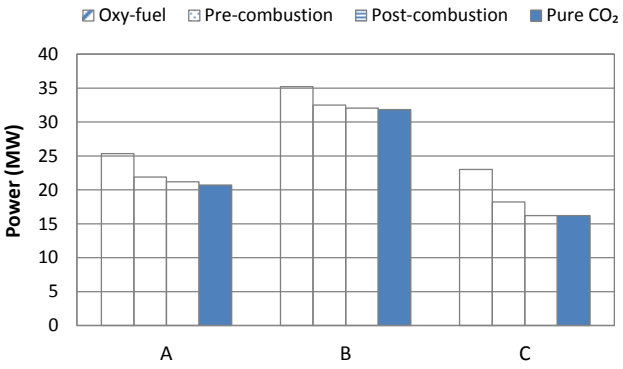

Figure 6. Power demand for multistage compression (options A, B and C) of pure CO_2, oxy-fuel (raw/dehumidified), pre- and post-combustion streams (compositions derived from Table 2).

Non-isothermal Steady State Flow Modelling

To evaluate the impact of CO_2 impurities on pressure drop in pipelines a computational model was developed to resolve steady state flow in networks, including the ability to account for multiple input sources with varying flowrates, compositions and fluid properties.

This involves the solution of the following conservation equations for mass, momentum, energy and component:

$$\frac{d(\rho u)}{dx} = 0 \tag{1}$$

$$\frac{d\rho u^2}{dx} = -\frac{dp}{dx} - f\frac{\rho u^2}{2D} - \rho g \sin\theta \tag{2}$$

$$\frac{d\rho u\left(h + {}^1/_2 u^2\right)}{dx} = \frac{4q_w}{D} - f\frac{\rho u^3}{2D} \tag{3}$$

$$\frac{dz_i}{dx} = 0,\ i = 1, \ldots, n. \tag{4}$$

where x, D, ρ and h are the local coordinate along the pipeline, the pipeline diameter, the density and enthalpy of the fluid respectively. u, P and θ respectively represent the velocity of flow, the fluid pressure and the angle of inclination of the pipeline with the horizontal axis. f and q_w are the Darcy friction factor and the heat flux at the pipe wall, the calculation of which can be found in Martynov et al. (2015). The model has been applied to study the impact of variation in the feed flowrate from sources as well as the concentration of impurities upon the pressure and temperature profiles along the pipeline and the delivery composition for a given temperature of the feed streams.

Figure 7 (a) shows an example of the considered realistic pipeline network transporting CO_2 from Cottam and Drax power stations to the sequestration point at Morecambe South in the East Irish Sea. While Figure 7 (b) shows the pressure drop along this main truck line assuming a total feed flowrate of 25 Mt y^{-1} as well as both an increase and decrease of 10 % from the Drax power station. In this case the CO_2 stream is a mixture of various impurities, including water, argon, nitrogen and oxygen, which are typically present in an oxy-fuel combustion CO_2 stream.

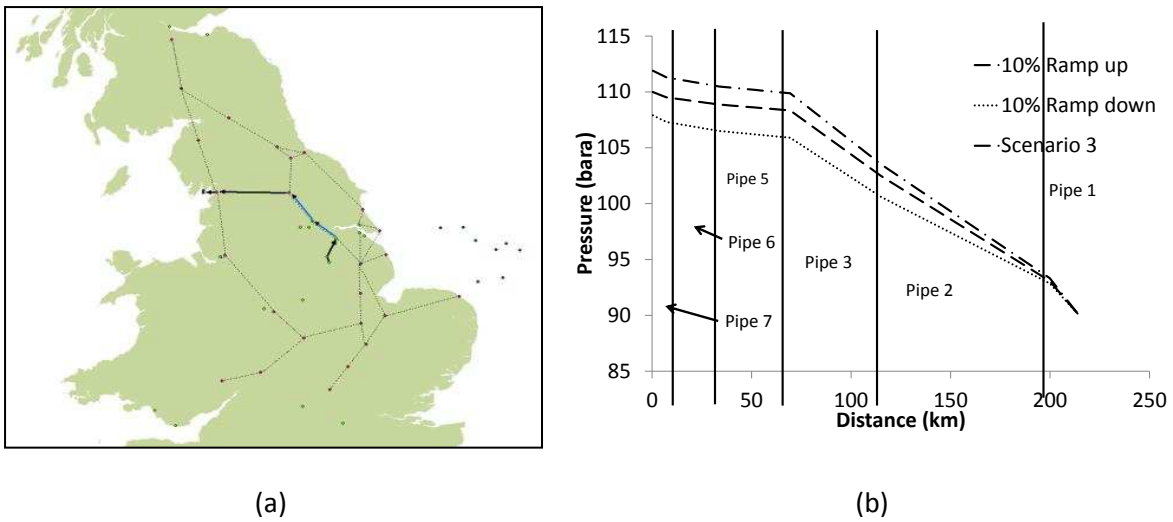

(a) (b)

Figure 7. (a) UK CCS pipeline transportation network, 2015-2025 (b) variation of fluid pressure along a main trunk pipeline for variations in the CO_2 flowrate from Drax power station (Brown et al. 2015).

As can be observed, in this case the alteration in the flowrate from just one of the CO_2 sources produces an increase in pressure drop of over 10 %. It has been found that variations in the feed composition can have a similar impact on the pressure drop even in this simplified case-study.

4.2 Small to medium scale pipeline releases

Medium-scale experiments involving high pressure releases of CO_2 containing a range of impurities from a pipe were performed at INERIS, France. The experimental rig and the measurement techniques were developed during the CO_2PipeHaz project (CO_2PipeHaz, 2009; Jamois et al., 2014). In CO_2QUEST, the same system was used to gain a better understanding of the influence of the presence of impurities on both the flow inside the pipe and on the external dispersion. The data were gathered for the validation of the mathematical models produced in CO_2QUEST.

The rig and equipment is shown in Figure 8. The pipe is 40 m long with a 50 mm internal diameter. Pressure (P), temperature (T) and heat flux transducers (F) were placed along its length at intervals of 10 meters. The pipe is thermally insulated. Calibrated orifices are placed at one end (6 mm or 12 mm - right hand side on Figure 8) while the CO_2 mixture is filled in

from the other end using a high pressure pump. The outflow near-field is also instrumented with pressure transducers and thermocouples (up to 50 cm from the orifice) to investigate the expansion zone. The measurement of the mass flow-rate is of great importance for the validation exercise of the models (Martynov et al., 2013). To do this, electronic measuring load cells were installed at six locations between the top of the supporting masts (in blue on Figure 8) and the bottom of the pipe. A transparent section is also installed in the middle section of the pipe to record video of the phase transition using a high speed camera. This also helps to check that the pipe is correctly filled. To produce "impure" CO_2 mixtures, the desired quantity of the chosen "impurity" (N_2 or CH_4 in this case) is injected in the pipe. The CO_2 filling is then completed to reach a pressure above the bubble point. The inventory is homogenously mixed by re-circulating the fluid through an external loop before experiments are carried out.

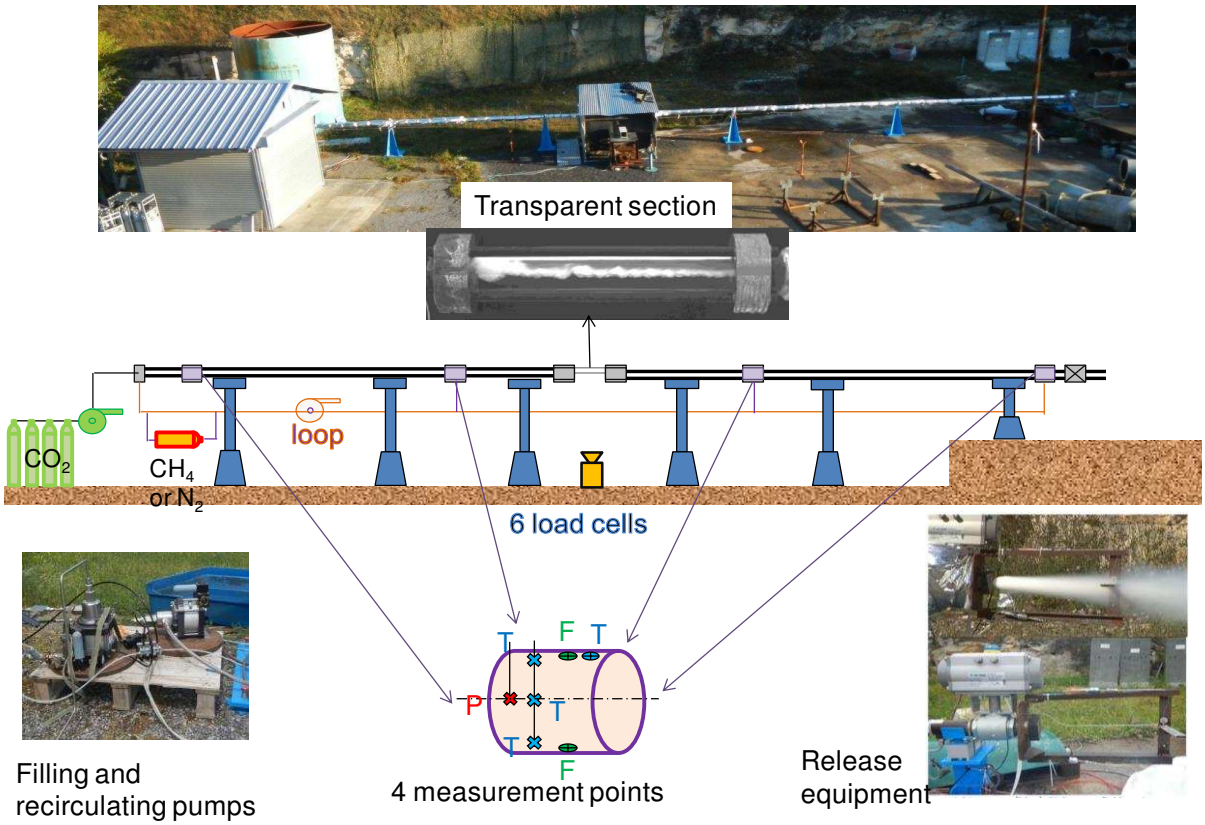

Figure 8. Presentation of the experimental rig constructed and operated by INERIS for "medium scale" CO_2 releases.

Twenty nine release experiments were performed varying the temperature and composition of the fluid and the diameter of the release orifice. Two experiments are discussed here to illustrate the experiments performed (Table 3): a 6 mm diameter release of pure CO_2 and a 12 mm diameter release with a CO_2+N_2+CH_4 mixture.

Table 3. Initial conditions of selected experiments.

Test n°		1	2
Mixture		**Pure CO_2**	**CO_2+2%N_2+2%CH_4**
Pressure	[Bar]	56	58
Ambient temperature	[°C]	17	10
Orifice diameter	[mm]	6	12

The mass flow rate is calculated using a temporal derivation of the measured mass (Figures 9 and 11).

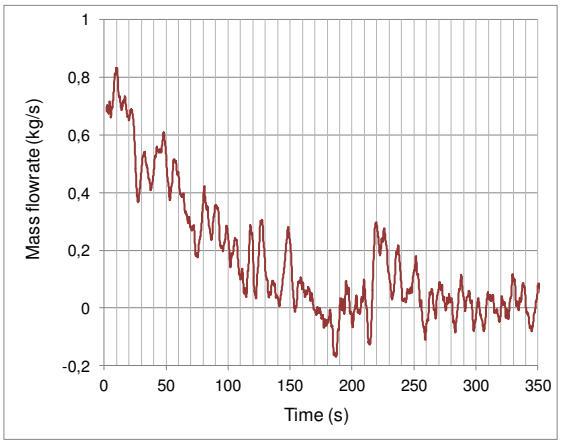

Figure 9. Mass flow rate (test 1:6 mm diameter, pure CO_2 release)

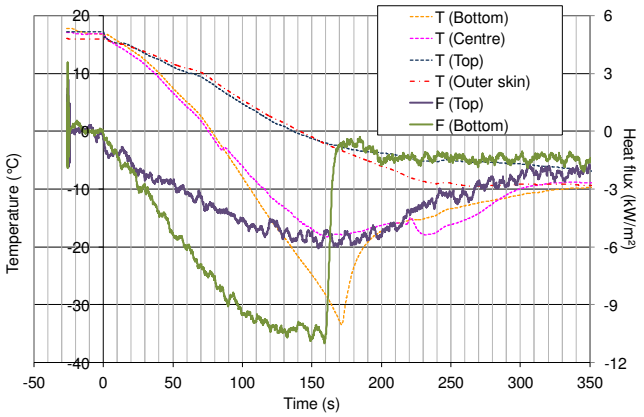

Figure 10. Temperature and heat flux measurements near the orifice during a 6mm diameter release (test 1: 6 mm diameter, pure CO_2 release)

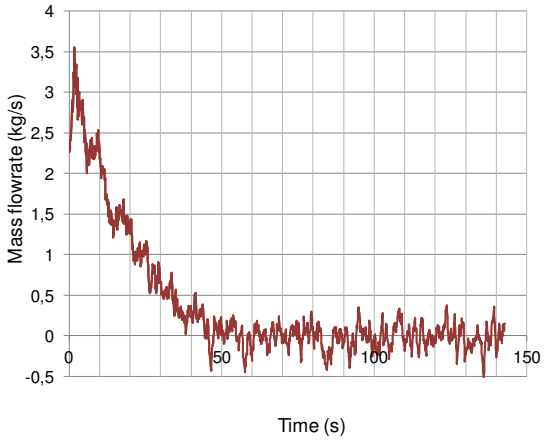

Figure 11. Mass flow rate (test 2: 12 mm diameter, CO_2+2%N_2+2%CH_4 mixture)

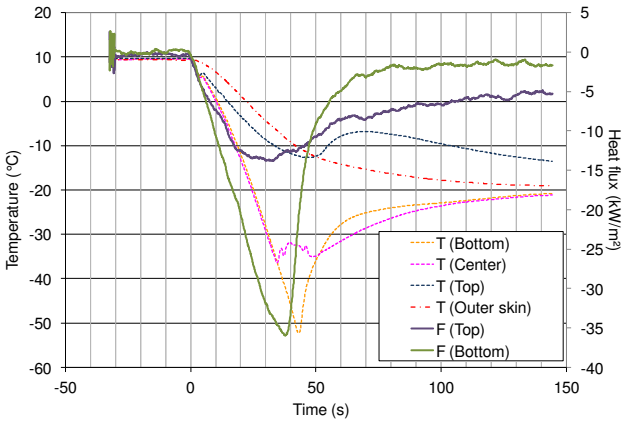

Figure 12. Temperature and heat flux measurements near the orifice during a 6mm diameter release (test 2: 12 mm diameter, CO_2+2%N_2+2%CH_4 mixture).

In both tests, during the first few hundred milliseconds of the release the fluid is nucleating but still seems homogenous. During the next period (until 23 s after the start of the release for test 1 and 4 s for test 2) a segregated two-phase mixture is present in the pipe but the level of liquid is above the orifice. The level of liquid reaches the orifice height 50 s after test initiation for test 1 and 12 s for test 2. After this the outflow becomes a gaseous jet. In the pipe the liquid disappears after less than 2 minutes for test 1 and approximately 35 s for test 2.

Further, modelling work often assumed pipe flow was adiabatic. An example of the evolution of the heat fluxes close to the orifice is shown in Figures 10 and 12. The various phases discussed above can be identified (liquid, two phase, gas). At the bubble point the heat flux

decreases abruptly while the temperatures remain almost constant suggesting a phase transition. This occurs earlier on the heat flux meters located on the top of the pipe where bubbles are forming. Subsequently the heat flux slope decreases in the gaseous phase (top of the pipe) while the slope remains much larger at the bottom, until the liquid is completely vaporized. This is certainly due to the vaporization of the liquid which absorbs energy from the metal of the pipe more rapidly than the vapour does due to its higher heat transfer coefficient. When the liquid is almost completely vaporized the thermodynamic conditions are close to the triple point and the heat flux measured at the bottom of the pipe decreases very abruptly and stays at a very low value until the end of the release, indicating no further vaporization is taking place. Contrariwise, the heat flux measured at the top of the pipe reverts to zero more slowly. This may be due to the conductive exchanges between the top and the bottom of the pipe through the thickness of the wall.

4.3 Large scale pipeline releases

The main objective of this section of the project was to conduct controlled large-scale experiments involving high pressure releases of CO_2 with a range of impurities. Experimental data recorded included near-field measurements of the dispersing jets and temperature measurements in the vicinity of a pre-designed crack geometry. This activity has provided experimental data that can be used to validate the CFD models developed as part of the project and described in the next section.

A fully instrumented industrial scale CO_2 pipeline was designed and built by Dalian University of Technology (DUT), China. The pipeline consisted of a main section with a length of 257 m and an internal diameter of 233 mm, a dual-disc blasting pipe with a length of 1 m, CO_2 injecting lines, a heating system (48 kW), a recoil force defender, a group of video recording systems and two data acquisition systems. Pressure and temperature data was recorded along the pipeline and in the dispersion area. Schematics of the pipeline are shown in Figure 13.

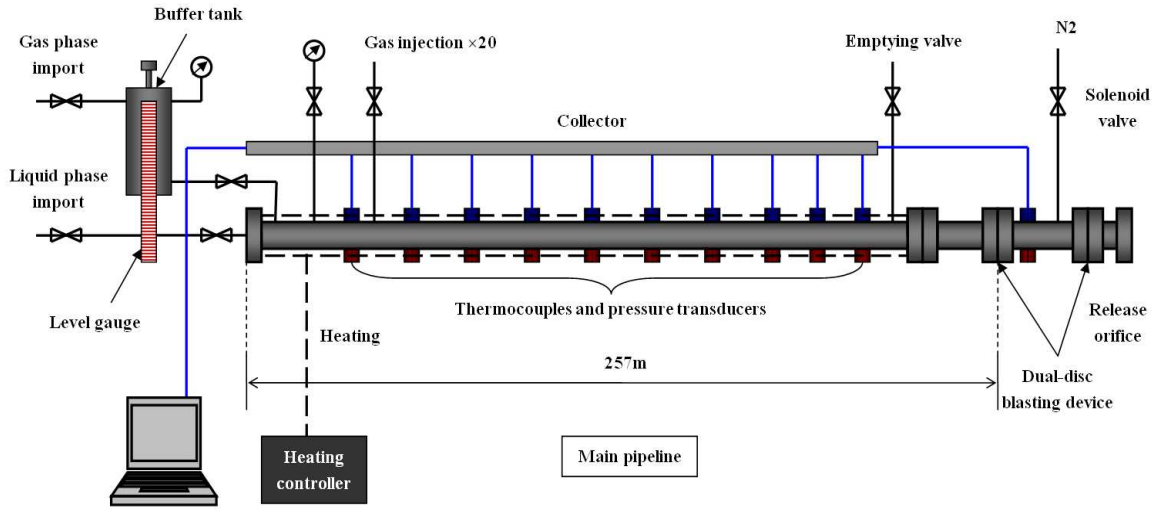

(a) Schematic diagram of the pipeline

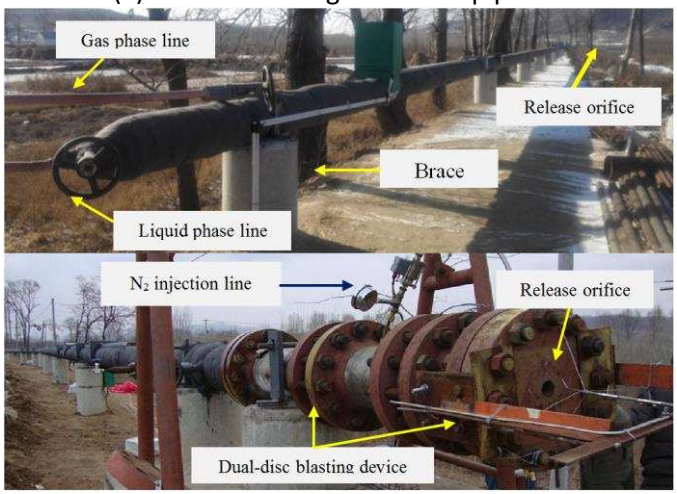

(b) Photograph

Figure 13. Schematic and real images of experimental apparatus.

Along the main pipeline, many pressure sensors and thermocouples were installed to monitor the pressure and temperature of the main pipeline and inventory during experiments. A large number of thermocouples and CO_2 concentration sensors were also arranged on vertical masts in the dispersion area at various distances from the orifice. Ten groups of CO_2 pipeline release experiments were performed with a range of impurities, initial inventory conditions and three discharge diameters including 50 mm, 100 mm and 233 mm (FBR). During release experiments the transient variation in fluid properties was recorded both in the pipeline and in the dispersion cloud. Additionally video recordings of the dispersing cloud were made from various locations, including from an overhead drone.

4.4 Near-field structure of, and heat transfer from, CO_2 releases

A computational fluid dynamic code developed under the EU FP7 project CO_2PipeHaz (http://www.co2pipehaz.eu/), capable of modelling the near-field structure and dispersion characteristics of releases of CO_2, has been extended to cover CO_2 mixtures with impurities and trace elements typical of those found in CCS streams. This includes both a continuous phase fluid model and a discrete-phase model capable of representing the distribution and properties of solid and liquid particles in such releases. The latter is an important consideration given the unusual phase behaviour of CO_2, and its sublimation from solid form at atmospheric conditions. The original model was based on solutions of the ensemble-averaged, density-weighted forms of the transport equations for mass, momentum and total energy. Closure of this equation set is achieved via the k-ε and Reynolds stress turbulence models corrected to accommodate the effects of compressibility. The use of a second-order accurate numerical solution scheme makes it possible to capture the detailed structure of the shock fronts that arise in accidental releases by using fine computational grids in the areas of interest. The computational cost of capturing such structures is reduced through the use of an adaptive mesh refinement (AMR) algorithm. AMR techniques have the advantage over uniform grids in physical space in that refined numerical solution meshes are only used at those points in a flow where significant change is taking place. Solutions are also calculated on each grid with a time step appropriate to that grid, with the whole refinement process controlled by using solutions to obtain an estimate of the truncation error. This approach is highly efficient since calculations in both time and space are performed only as required by the dictates of local numerical accuracy. Integration of the equations employs a second-order accurate finite-volume scheme in which the transport equations are discretised following a conservative control-volume approach. Approximation of the diffusion and source terms is undertaken using central differencing, and a Harten, Lax, van Leer second-order accurate variant of Godunov's method applied with respect to the convective and pressure fluxes. The complete model has been validated, e.g. Woolley et al. (2013), against experimental data obtained in a number of release scenarios including data on free jet releases and releases representative of punctures and ruptures of buried high pressure pipelines. It has also been demonstrated as part of an integrated, multi-scale modelling approach for the simulation of multi-phase dispersion from accidental CO_2 pipeline releases in realistic terrain (Woolley et al., 2014).

The model described above contains a composite equation of state (Wareing at al., 2013) for predicting the thermodynamic physical properties of carbon dioxide above and below the triple point, in all three phases (solid, liquid and gas) and at all phase changes, including the latent heat of fusion. In the present project the overall model is being extended to permit the dispersion characteristics of CO_2 and its impurities to be handled through the consideration of multiple scalars, with the effect of impurities on the thermodynamic physical properties accommodated using the equation of state developed by NCSR and that embodied in the TREND software package of Span et al. (2015). These provide relevant phase equilibrium and thermophysical data covering the range of impurities, operating pressures and temperatures applicable to the entire CCS chain. The presence of even small amounts of impurities can have a significant effect on the phase behaviour of CO_2 mixtures and must be considered as they account for changes in critical pressures and temperatures. The overall model is being validated against experimental data generated at different scales by project partners INERIS and DUT to demonstrate its usefulness for risk assessment purposes. Example predictions of the impact of impurities on near-field predictions of pure and impure releases are shown in Figure 14.

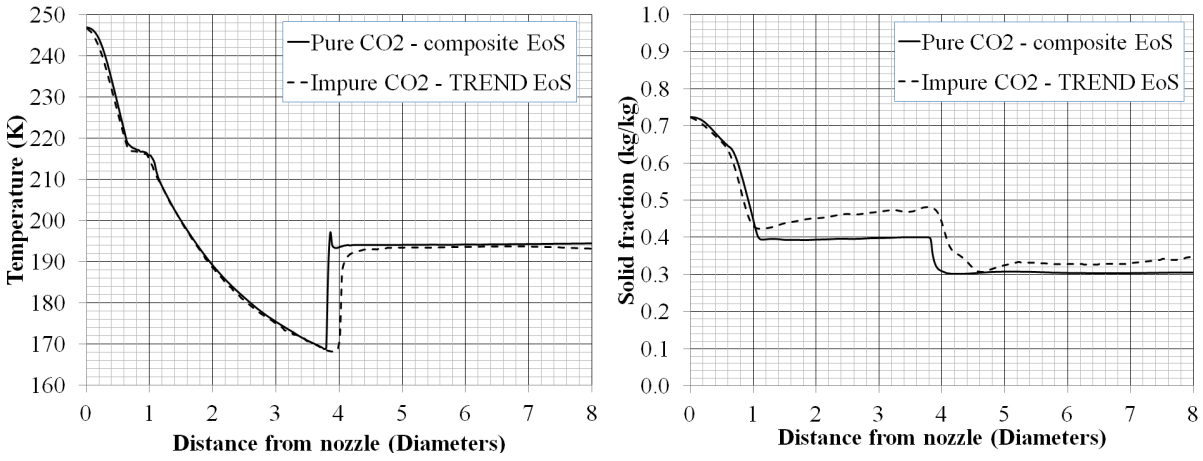

Figure 14. Shown are pure (100% CO_2) and impure (96% CO_2, 4% N_2) predictions of temperature (left) and solid fraction (right) in a near-field dispersion calculation, using a composite equation of state for the pure calculation (Wareing et al., 2013) and TREND 2.0 with solid CO_2 modifications for the impure calculations.

Further development of the model has also been undertaken to extend its capabilities to predict the heat transfer characteristics observed between a dense liquid release of CO_2

expanding through a puncture in a pipe and the pipe walls. Such an ability allows the prediction of crack-tip temperatures and pressures which can then be incorporated into crack propagation models, considered elsewhere in the project, to predict the propensity for a particular release scenario to escalate into a catastrophic incident due to running brittle fracture. It has been shown (Mahgerefteh and Brown, 2011) that changes in pipeline temperature by as little as 10° C can result in the transformation of a short crack into a fast-running long fracture, and it is anticipated that Joule-Thomson cooling will be affected by the presence of impurities in a release. The model described above was coupled to an appropriate transport equation for heat transfer in the solid pipe, using the thermophysical properties of typical pipeline steel, with the predictions of the complete model compared with data gathered by INERIS. Figure 15 shows the experimental set-up and associated computational details, together with model predictions of the velocity field outside the pipe. Table 4 demonstrates reasonable agreement with experimental temperature data at different times during a release of pure CO_2 at 277 K and 5.30 MPa for two of the thermocouple locations indicated in Figure 15(a). Similar levels of agreement were found at other measurement stations and in other tests.

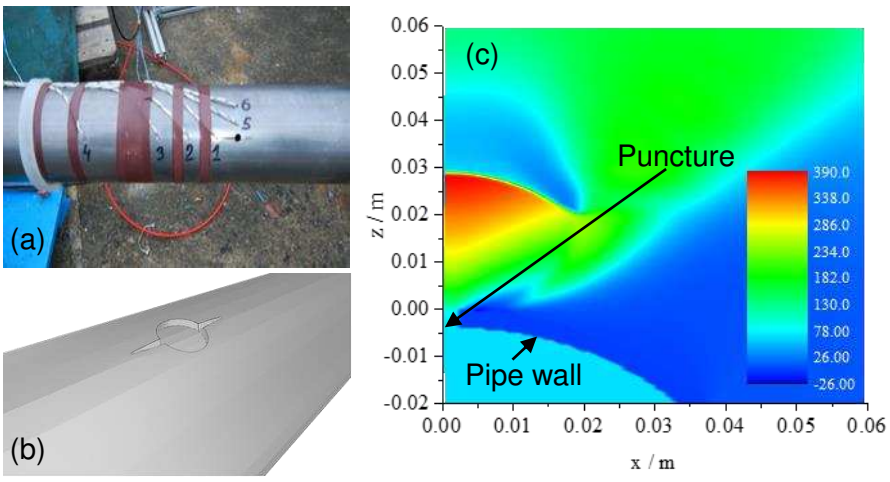

Figure 15. (a) Experimental rig showing thermocouple locations, (b) three-dimensional representation of the puncture and associated cracks, and (c) total velocity predictions at the puncture exit (in m s^{-1}).

Table 4. Comparison of experimentally observed and predicted pipe surface temperatures at three times during a release.

Time / s	Temperature / K			
	Thermocouple 2		Thermocouple 3	
	Measured	Predicted	Measured	Predicted
1	267	274	274	274
125	269	264	271	264
250	258	256	259	256

4.5 Brittle and ductile fracture tests and associated modelling

Material Selection

Different experiments were performed in order to compare the behaviour of three different steel grades that can be used for CO_2 pipelines. Steel grades X65, X70 and X80 have been compared under dynamic loading conditions. Firstly, Charpy V-Notch (CVN) and Drop Weight Tear Test (DWTT) experiments were carried out to monitor Ductile to Brittle Transition Temperature (DBTT) curves at different temperatures ranging from 20°C to -80°C. Based on performed dynamic fracture experiments it has been found that the X70 steel offers the best combination of strength, low temperature toughness and resistance to (accidental) H_2S exposure as depicted in Figure 16.

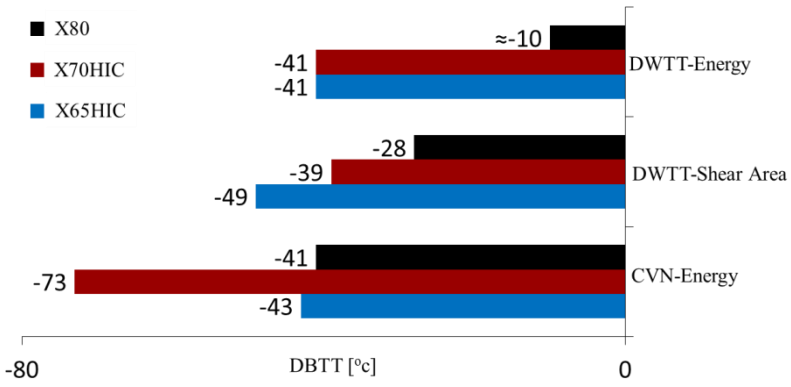

Figure 16. Comparison of DBTT between three steel grades X65, X70 and X80 according to CVN and DWTT.

Ductile model

The present study develops a fluid-structure coupling methodology for simulation of scenarios of pipeline failure involving ductile and brittle fracture propagation. To simulate the state of the fluid in the rupturing pipeline a one-dimensional compressible CFD model is applied. The proposed methodology couples the CFD model describing the pipeline decompression (Mahgerefeh et al., 2006; Brown et al., 2015) and the Modified Bai-Wierzbicki (MBW) material damage model (Döbereiner and Thibaux. 2013; Talemi et al., 2016a), which has been implemented in the Finite Element Analysis (FEA) code ABAQUS. The coupled fluid-structure ductile fracture model has been validated against experimental data reported in the literature on fracture propagation in a large-scale X70 pipeline (Makino et al., 2004).The developed coupled fluid-structure model was applied to simulate a full-scale burst test, showing that the coupled approach is capable of predicting the real fracture behaviour of pipeline steels under different dynamic loading conditions relevant to running fractures in real-scale high-pressure pipelines.

Figure 17 (a) shows the variation of the crack velocity with the crack length as predicted using the coupled fluid-structure fracture model (MBW+CFD) employing various numbers of cells in the CFD code with predictions using the HLP model and the experimental data. Figures 17 (b) and (c) show a photograph of a fractured pipeline taken from (Makino et al., 2004) and predicted corrugated deformation using the coupled fluid-structure fracture model, respectively.

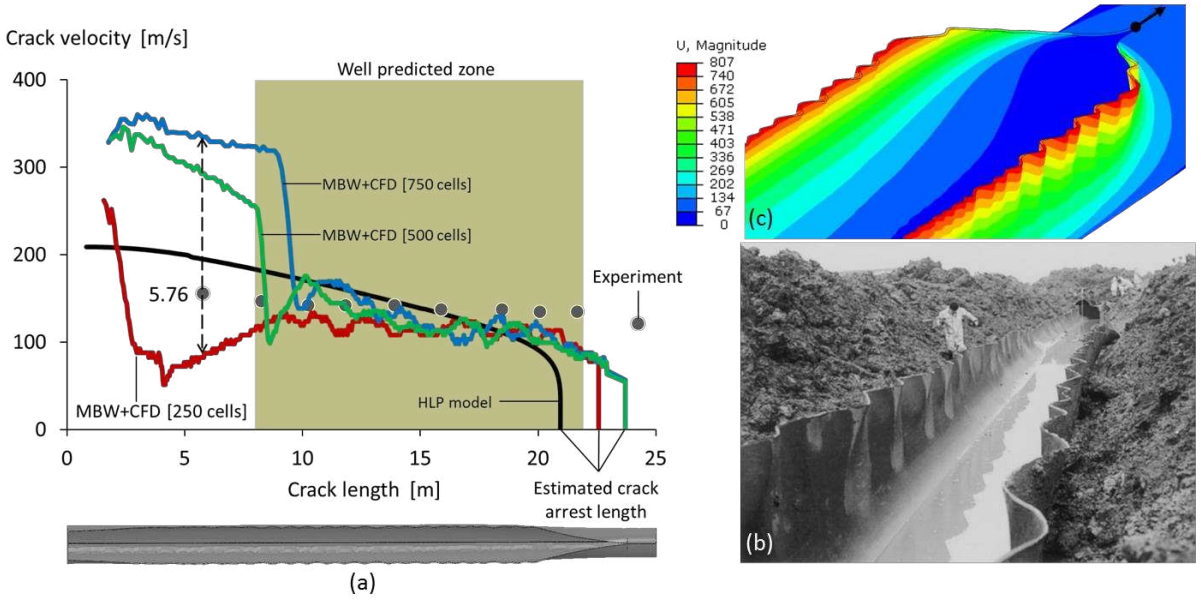

Figure 17. (a) Predicted crack propagation velocity by the MBW+CFD model and the HLP model in comparison with prolonged release experimental observations, (b) Photograph of a fractured pipeline taken from (Makino et al., 2004) and (c) predicted corrugated deformation using the coupled fluid-structure fracture model.

In terms of the brittle fracture model, a novel approach of the eXtended Finite Element Method (XFEM)-based cohesive segment technique has been used to model dynamic brittle fracture behaviour of pipeline steel (Talemi et al., 2016b). In this model the dynamic stress intensity factor and crack velocity are calculated at the crack tip at each step of crack propagation. To calibrate the brittle fracture model data from lab-scale experiments i.e. CVN and DWTT of X70 pipeline steel at low temperatures has been applied (Talemi, 2016). Using the methodology developed i.e. a hybrid fluid-structure modelling approach, a study is performed to evaluate the impact of CO_2 fluid phase and pipeline transportation conditions on the rate of brittle fracture propagation in a real-scale 48" OD pipeline. The model allows the quantitative prediction of the pipeline tendency to long running fractures in the form of the variation of crack length with crack velocity.

5. WP3 – EFFECTS OF IMPURITY GASES IN THE CO_2 STREAM ON ITS GEOLOGICAL STORAGE

The effect of impurity gases on the geological storage of CO_2 is studied in the CO_2QUEST project by a suite of methods ranging from laboratory and field experiments to predictive modelling and related model development. Two major field experiments are being carried out. In the first, supercritical CO_2 along with selected impurity gases is injected into a reservoir layer at a depth of 1600 m, the effects of such an injection on measurable quantities, such as pressure, temperature and in particular the chemical composition of the resident water will be investigated. Laboratory experiments are carried out on rocks from this site to investigate the effects of impurity gases on rock composition and to allow comparison between the laboratory and field results. In the second field experiment the focus is on scenarios mimicking potential CO_2 and impurity gas leakage into shallow aquifers. In this experiment industrial grade CO_2 is injected into a shallow water aquifer, followed by the monitoring of the injected fluid, its trace impurities and the potential mobilization of metallic trace elements from the surrounding rock. The modelling work has two main objectives; (i) to plan, predict and interpret the field experiments in order to gain understanding of the relevant processes happening in-situ and (ii) to make long-term predictions on the effect of impurity gases in large scale storage scenarios. In the following sections we will discuss some of the key aspects of the project and present some example results.

5.1 Deep CO_2 injection experiment at Heletz site, Israel

The Heletz site in Southern Israel has been developed for scientifically motivated CO_2 injection experiments with the objective of improving our understanding of the fate of geologically stored CO_2 in situ, in particular CO_2 spreading and trapping processes and developing methods for quantifying them from measurable quantities such as pressure, temperature and fluid samples. Extensive site characterization has been carried out and is summarized in Niemi et al (2016a; 2016b). The first of the planned CO_2 injection experiments are described in Fagerlund et al. (2013) and Rasmusson et al. (2014)) and will address in-situ measurement of residual and dissolution trapping of pure CO_2. These will be followed by experiments related to the effects of impurity gases in the injected CO_2 stream.

The site is located East of the city of Ashkelon (Israel) at the eastern edge of a depleted oil field. The target formation "the Heletz sands" comprises three sandstone layers "K", "W" and "A", having a cumulative thickness of ~10 meters. Above the reservoir, there is a caprock of ~ 40 m thickness mainly composed of shale and marl. The site was prepared as part of the EU-FP7 MUSTANG (coordinated by Uppsala University) and TRUST (coordinated by EWRE) projects. It comprises:

1. Two deep wells penetrating the reservoir to a depth of 1650 meters: well H18A, which is instrumented for CO_2 injection, fluid abstraction (via airlift), downhole pressure and temperature monitoring, downhole fluid sampling, Digital Temperature Sensing (DTS) via an optical fiber and chemical injection (for CO_2 saturation of water, tracer injection and impurities injection); well H18B, which is instrumented for fluid abstraction (via airlift), downhole pressure and temperature monitoring and DTS. The distance between the wells is 50 meters.
2. Three shallow wells (to a depth of ~250 meters): H18SA, H18SB and H18SC. These wells are intended for seismic monitoring of the injected CO_2 body.
3. A CO_2 injection kit (Figure 20): low flow (for CO_2 water saturation) and high flow (for CO_2 injection) pumps (Figure 19), a heat exchanger (Figure 18, for controlling the temperature of the injected CO_2) and a CO_2 storage tank. This kit is heavily monitored (P/T sensors long the path from the CO_2 tank to the wellhead) and is operated in semi-automatic mode.
4. A high pressure – high discharge air compressor for fluid abstraction via air-lift.
5. A high pressure nitrogen booster used for lifting fluid samples and purging of the injection system between injection sequences.
6. A control room to which all the monitoring technologies converge (including the seismic monitoring, measurements from the CO_2 tank, the wellhead and downhole measurements and the fluid samples). Facilities for onsite fluid characterization (including high pressure pH and EC measurement, mass spectrometer, alkalinity) are installed and integrated.
7. A line for the co-injection of CO_2-SO_2 and CO_2-N_2.

So far, the extensive characterization activities that have taken place include:

1. Geophysical logs conducted in both wells which have identified the target layers and the caprock.
2. Laboratory analysis of reservoir and caprock cores for mineral characterization, porosity/permeability measurement, hydro-mechanical characterization and chemical reactivity (carried out by CNRS-France, LIAG and Göttingen University

(Germany), Edinburgh University (Scotland). Impact of impurities at core scale has been investigated by CanmetENERGY of Canada.

3. Baseline Seismic survey, conducted by the Geophysical survey of Israel (GSI).
4. Hydrogeological characterization via pumping tests conducted in the wells. These show that the reservoir properties are rather favourable (permeabilities of ~720 mD).

The injection CO_2 system has been verified and successfully commissioned.

Figure 18. The heat exchanger.

Figure 19. Pump skid during commissioning.

Figure 20. Connection to the injection well.

5.2 Shallow CO_2 injection experiments at Catenoy site, France

INERIS conducted an injection experiment of industrial grade CO_2 into a shallow aquifer in order to simulate a vertical leak that is supposed to occur from deeper storage in a saline formation. A site for this experiment has been selected and equipped by INERIS in the chalky aquifer of the Paris Basin (France). Located at Catenoy (Oise), it contains 4 air-wells (wells dedicated to underground atmosphere measurement and sampling in the unsaturated zone) and ten piezometers (wells dedicated to water table measurement and groundwater sampling in the saturated zone), seven of which are represented on Figure 21. The well W2b was drilled in the frame of the CO_2QUEST project.

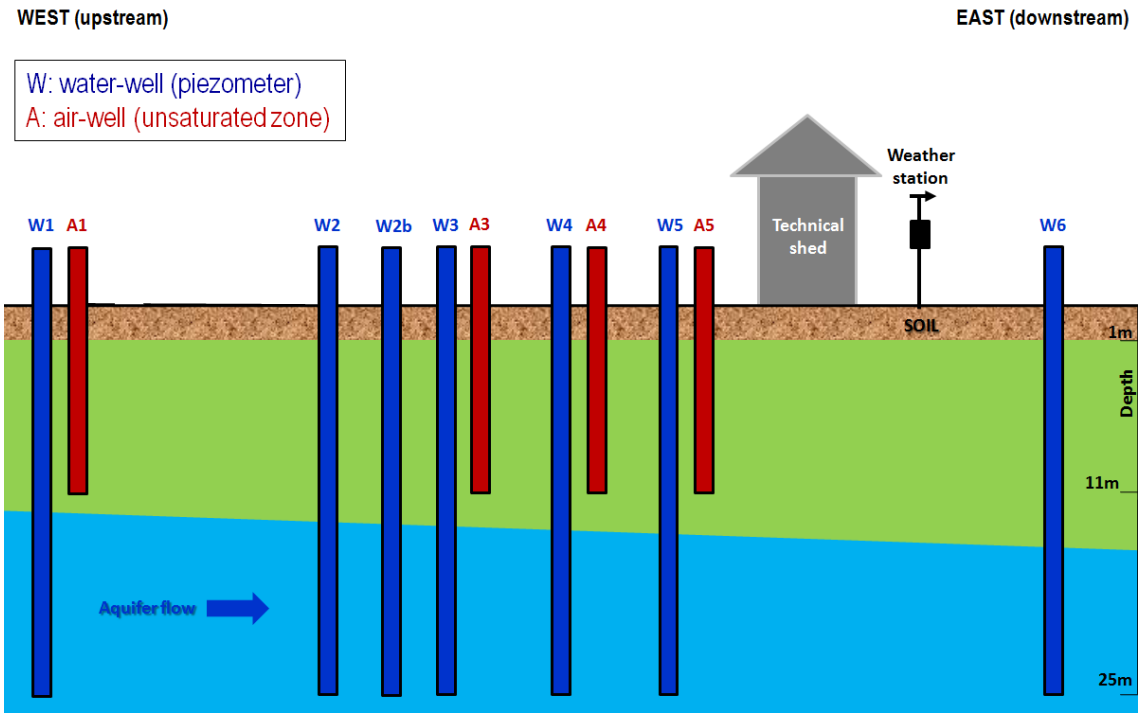

Figure 21 Cross section of the experimental site of Catenoy (W2b is the new well drilled in the project).

This experiment was a "push-pull" test that began with a 3-hour "push phase" in which 3 m^3 of brine containing salt, dissolved CO_2 and impurities was injected, followed by the "pull" phase which consisted of pumping water back from the aquifer between 3 and 7 days after the push phase. This water was analysed and in situ monitoring was performed in the neighbouring wells, both in the water and in the gas phase above the water table.

A number of observations were made from this experiment:

- the injected plume was observed 5 m downstream during the "push phase"
- pH lowered by about 0.5
- the maximum concentration of dissolved CO_2 increased to 0.1 g/L
- the maximum concentration of certain metals increased to 0.5 mg/L for Zn, 0.2 mg/L for Li and 0.01 mg/L for As as shown on Figure 22.

Gaseous impurities were also observed in the unsaturated zone above the aquifer at the same time (CO_2 concentration increased to 600 ppm and He to 8 ppm). Additionally, during the pull phase more prolonged but less significant increases of some impurities were observed

e.g. dissolved CO_2 increased to 0.04 g/L and Li to 30 µg/L. It was also observed that He no longer degassed even when still present in the water and Zn concentrations remain below the detection limit.

There is an obvious buffer effect in the chalky aquifer due to calcite dissolution. By running simulations of the geochemistry with the PHREEQC code we concluded that experimental and modelled Zn concentrations were in very good agreement during the push phase (see the peak on Figure 22) but during the pull phase it was assumed that in situ measurements were under the detection limit while the model over predicts Zn concentrations at low levels. Compared with other studies conducted by INERIS and with others from the literature this suggests that adsorption of iron oxides plays a key role in the transport of Zn and other metallic impurities. Future models will have to take this effect into account.

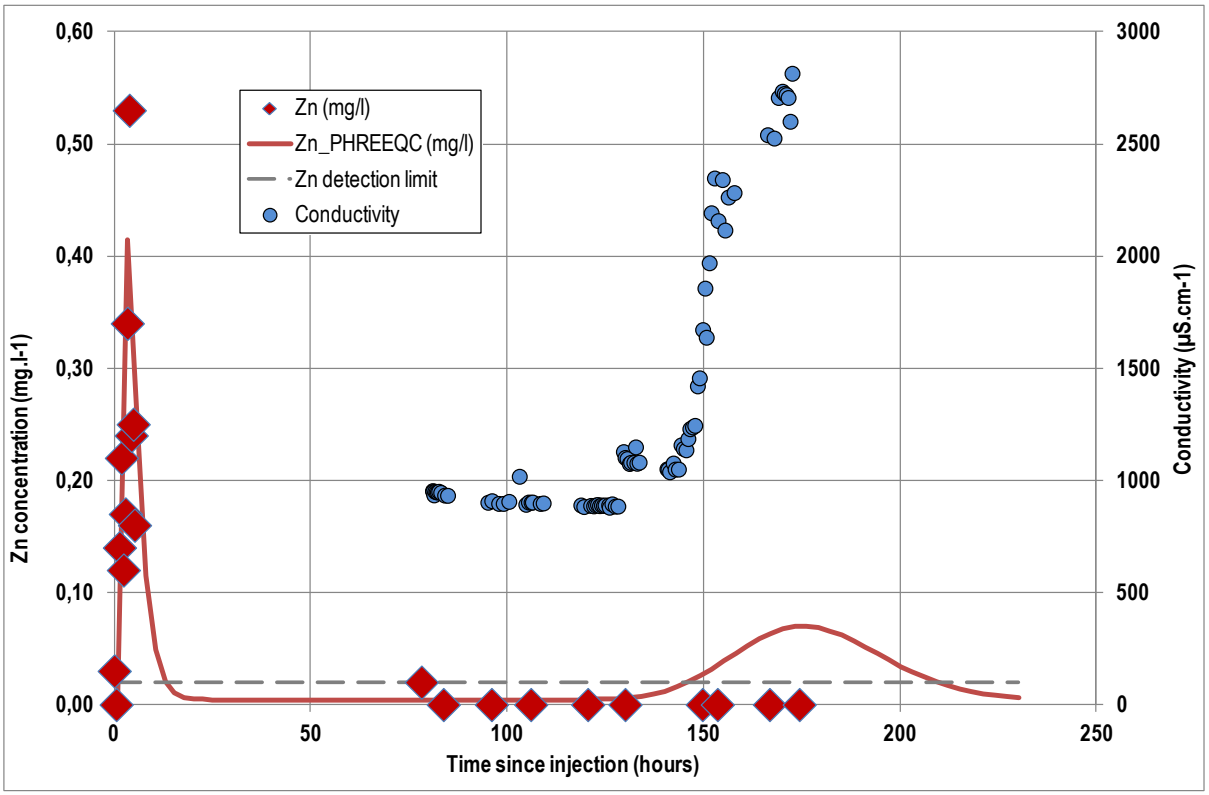

Figure 12. Experimental and simulated concentrations for Zn at well W2b, located 5 m downstream of the injection well.

These results indicate that the impact in the aquifer is very limited both for CO_2 and the impurities injected. After several days the impact is not noticeable further than a few dozen of meters. However, this result depends on the conditions of this field experiment. In order to

simulate a leakage from a storage located in a deeper geological formation it would be useful to perform an injection test for a longer period.

5.3 Modelling of CO_2 and impurity gases spreading in geological formations

Based on the review of the characteristics of impurity gases in the CO_2 stream and their potential impact on geological storage, two impurity gases were selected for the field experiment at Heletz; N_2 as it is expected to have a hydro-mechanical impact on gas/supercritical CO_2 flow and SO_2 for its expected geochemical impact. In the following sections their predicted effects are discussed.

5.3.1 Modelling of the hydrodynamic processes affected by impurity gases

The hydro-mechanical modelling of the spreading of a CO_2-rich phase was based on the well-known TOUGH2 simulator (Pruess, 2004). TOUGH2/ECO2N code as such is capable of simulating multiphase flow migration and mass partitioning of H_2O and CO_2 in both brine-rich and CO_2-rich phases (Pruess and Spycher, 2007). Solid salt precipitation is also considered, dissolution/precipitation is calculated using local equilibrium solubility. However, the effect of multiple gases in the gas/CO_2 rich phase is not accounted for. For the purpose of modelling the effect of impurity gases the EoS included in the code was updated here. In this we follow the approach of Fagerlund and Niemi (2007). We assume the CO_2 rich phase to be a mixture of CO_2 and the impurity gases of interest. The movement of the gas phase, which depends on phase properties like density and viscosity, is governed by the properties of the gas mixture. In our numerical implementation we allow the composition of this gas mixture to be continuously updated with time as the different gases of the mixture dissolve into brine at different rates according to their specific solubilities. With this approach we assume that the gas mixture consisting of CO_2 and impurities does not separate within the gas phase itself and can therefore be treated as a so-called pseudo gas mixture representing the fluid properties of the mixture as calculated from the updated EOS.

In practice this is implemented into the TOUGH2 code as follows: during the simulation, we first compute the mass fractions of the different gases in the gas mixture. We then calculate the gas properties of each component gas, for example, compressibility factor, fugacity, and solubility of each gas into the brine phase by using the thermodynamic equations developed

by Duan and Mao (2006) and Duan et al. (2007). We then calculate density, viscosity and enthalpy of the gas mixture. These physical properties are determined by the external program REFPROP developed by U.S. National Institute of Standards and Technology (NIST). This program uses Kunz and Wagner models for gas mixtures (Kunz et al., 2007). After advancing a time step dissolved mass in the brine will be subtracted from the initial gas contents and the mass of each gas is updated for the next time step.

Hydro-mechanical impacts of CO_2 and N_2 co-injection

The modified TOUGH2/ECO2N code was used to model the reference push-pull CO_2 injection experiment at Heletz (Rasmusson et al, 2014) and to predict what effect the N_2 gas would have on the experiment result. N_2 was chosen as the example impurity gas for these simulations as it can alter the density and viscosity of the CO_2 plume significantly, thereby giving an estimate on the physical influence of impurities on pressure and migration while not reacting chemically with the target formation. The experiment described by Rasmusson et al (2014) is simulated and the pressure response and plume migration of the pure CO_2 case is compared with that of gas mixtures with an N_2 content of 5 % to 10 %. The simulated test sequence with pure CO_2 is presented in Rasmusson et al. (2014). Here we simulate the early part of this test sequence both with and without N_2 in the CO_2 stream in order to estimate how the physical transport processes will be impacted. In this sequence we first inject pure CO_2 for the sake of reference and then co-inject CO_2 with a 5 % to 10 % mass fraction of N_2 to compare the respective hydro-geologic responses on key variables such as pore pressure evolution and plume migration.

The temporal variation of pore pressure during the simulated experimental sequence is shown in figure 23. In all cases pressure increases during water injection and decreases following mass production. The pore pressure rises again during the co-injection of CO_2 and N_2, then drops and stabilizes after injection. In general, a higher pressure is observed when a larger N_2 content is applied, with 10 % and 5 % of N_2 creating overpressures (in comparison to the pure CO_2 case) of about 450 kPa and 225 kPa, respectively. The density decrease of the gas mixture also impacts the plume migration. By increasing buoyancy the plume becomes lighter and moves further compared to the pure CO_2 case (figure 24). Mixing N_2 with CO_2 decreases the viscosity of the resulting gas mixture which eventually affects the mobility of the gas phase because the hydraulic conductivity is inversely proportional to the viscosity.

Solubility changes of each gas component in the brine phase were also investigated. After CO_2 and N_2 injection for 12 days, the CO_2 mass fraction in brine increases up to ca. 4.7 % in the case of pure CO_2 but only to about 4.5 % with an N_2 content of 10 %. N_2 solubility is directly proportional to initial content in the gas mixture and increases up to about 0.012 % when 10 % of N_2 is co-injected. The simulation results showed a linear correlation with initial mass ratios of gas mixture because the solubility of a gas component into brine is primarily controlled by the partial pressure of each gas in the gas mixture. Overall however, the hydrodynamic/hydro-mechanical effects are relatively small and we can expect greater impacts on geochemistry with different impurity gases, this will be discussed in the following section.

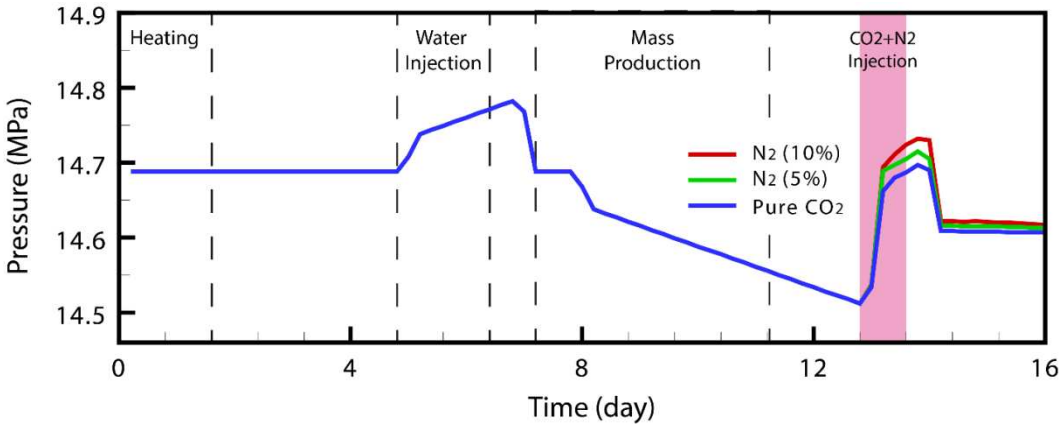

Figure 23. Temporal variation of the pore pressure during the push-pull experiments with the schedule suggested in Table 2. In all cases, pressure increases during the water and CO_2+N_2 injection and it shows a higher increase when the concentration of the impurity is higher. Note that the red line represents the 10 % N_2 case, green the 5 % and blue the pure CO_2 case (Rebscher et al., 2014).

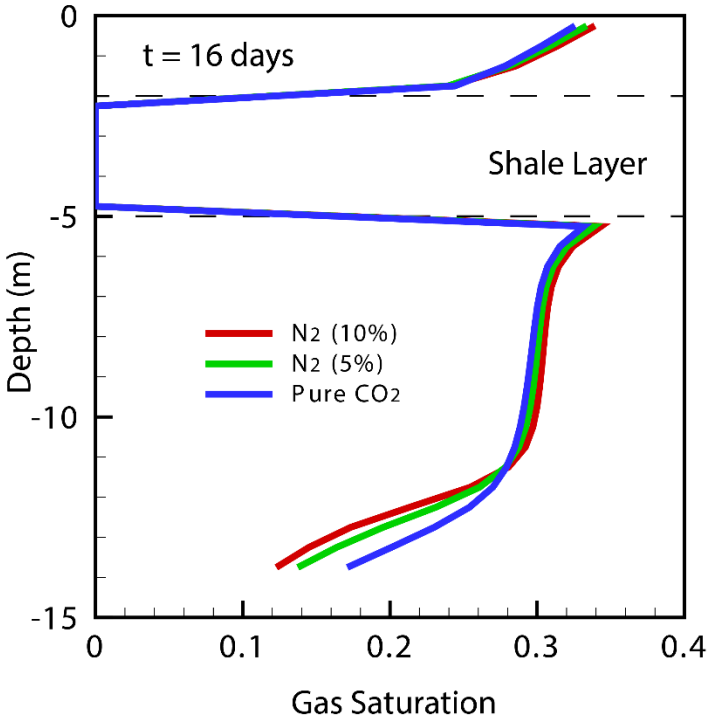

Figure 24. The depth profile of gas saturation at t = 16 days after the push-pull experiment. The plume shape from higher N_2 contents shows faster migration and move further upward because of density and viscosity decreases in the gas mixture (Rebscher et al., 2014).

Model for the geochemical effects

In addition to the impact of inert gases in a CO_2 stream it is of interest to analyse the effects of geochemically active impurities, both on the reservoir rock and on the caprock. Again Heletz data was used based on detailed mineralogical and petrophysical data provided by Edlmann et al. (2016) and Niemi et al. (2016) for the parameterisation of the generic models. These 1D and 2D radial models represent a sequence of the reservoir complex i.e. sandstone, shale, sandstone under a caprock, at reservoir scale. The 2D radial model covers a height of 16 m and a radial distance of 30 km, measured from the injection well. For the numerical simulations the coupled thermal, hydrological, chemical code TOUGHREACT V3.0-OMP from Lawrence Berkeley National Laboratory (Xu et al., 2014) was applied. This recent version features the special ability to implement transport of additional trace gases within the CO_2 rich phase. The study discussed in Wolf et al., (in prep.) is one of the first addressing SO_2 and NO_2 as a trace gas in the CO_2 stream, hence providing a significant contribution to understanding the impact on deep geological storage of impurities within a CO_2 stream.

The injection scenario discussed here consists of co-injecting CO_2 and SO_2 with a ratio of 99 % to 1 % at a constant rate of 9 kg/s over a period of 10 years. The numerical simulations demonstrate a preferential dissolution of SO_2 in the brine causing a strong reaction with the carbonate phases. Whereas the SO_2 is limited to the region of the bottom sandstone, CO_2 migrates through the intermediate shale layer and spreads in the upper sandstone along the contact with the caprock about a radial length of 80 m. Spatial differences of the impact of the two gases are obvious in the range of the lateral impact on the bottom sandstone. At the end of the injection period maximum horizontal distances of less than 200 m and about 2000 m were reached by SO_2 and CO_2 respectively in the case described.

Naturally changes in porosity are not only dependent on the fluid injected but also on the minerals present in the reservoir. In the Cretaceous sand layers at Heletz the initial porosity of the bottom sandstone layer is approximately 15 %. The dissolution of ankerite associated with the precipitation of anhydrite leads to a net porosity increase of about 0.5 %. Noteworthy is the self-sealing effect of the shale layer which is induced by the intrusion of SO_2 leading to a conversion of calcite to anhydrite. Here the decrease in porosity at the border between the lower sandstone and the intermediate shale layer amounts to a value of 1 %. But as the initial porosity of the shale layer was assumed to amount to less than 10 % this relates to a significant decrease in permeability. This stresses the importance of including chemical aspects while investigating thermal and hydrological processes and the necessity of site-specific evaluation, for further details see Wolf et al., (in prep.).

Long-term effects

Modelling of the laboratory and field experiments will enable model validation. Such validated models can be used with better confidence to make long-term and large-scale predictions. Even in the long term the processes of geochemical alteration and changes in two-phase flow properties discussed above will be important. An additional aspect is how impurity gases may influence dissolution and density driven convection, a process known to enhance solubility trapping. We investigate this effect for several co-contaminants (N_2, CH_4, and H_2S) by accounting for the impurity effects on both gas solubility and induced density changes driving the convective mixing. The study is conducted using multicomponent density-driven flow simulation with the USGS SUTRA-MS model which accounts for the relationship between a dissolved specie's mass fraction and the density change of the aqueous

phase, as well as the impact of dissolved CO_2 on the aqueous phase viscosity. Effects of impurities on the convective mixing are studied specifically in regard to the changes in onset time of convection, dissolution rate, flow pattern and solute distribution. The results show that the impurities investigated have the potential to reduce the convective mixing and the enhanced solubility trapping of CO_2. However, the effects on the convective mixing are limited due to the relatively small concentrations of impurities found in field.

6. WP4 – FULL CHAIN CCS TECHNO-ECONOMIC MODELLING

In this section we present a techno-economic analysis of gas purification and compression for CO_2 capture, shared capture infrastructure and CO_2 transport networks.

CO_2 Compression and Purification Units

Oxy-combustion capture is currently one of the most promising methods of CO_2 capture as it is one of the most developed and technologically mature methods for CCS. Unlike other mature technologies, oxy-combustion capture presents a trade-off between cost and purity. Oxy-combustion capture consists of an air separation unit (ASU) that produces a high purity oxygen stream and, mixed with recycled flue gas, provides a high-oxy environment in which to burn the fuel. The flue gas produced by oxy-fuel combustion will vary in purity depending on the input conditions and still requires dehydration, further purification and compression in order to be suitable for transport and storage. The latter is performed by means of a CO_2 Compression and Purification Unit (CO_2CPU).

In this work we have modelled four variations of the CO_2CPU in Aspen HYSYS using a Peng-Robinson property method with each system varying in their method of separation. These models were based on similar models presented by Posch and Haider (2012). The four models in order of descending complexity are: a CO_2CPU with a 6-stage distillation column, one with a double flash system with heat integration, one without heat integration and the least complex with only compression and dehydration. The results from these models show that an increase in product purity and complexity results in a reduction in capture efficiency. The capital and operational cost results for each CO_2CPU modelled were translated into a price for the CO_2 product stream shown in figure 25. In order to derive a price for each product it was assumed that the CO_2CPU is an independent entity in which to invest, with

two inlet streams - raw flue gas (free) and energy (cost) - and two outlet streams - CO_2 product (revenue) and waste stream. Figure 25 shows that at four different minimum rates of return (equated to the internal rate of return IRR) we find a non-linear and non-monotonic relationship between CO_2 price and purity. The difference between the highest purity product at 99.98 wt.% CO2 and the lowest purity product at 82.91 wt.% CO2 represents a 42% reduction in price.

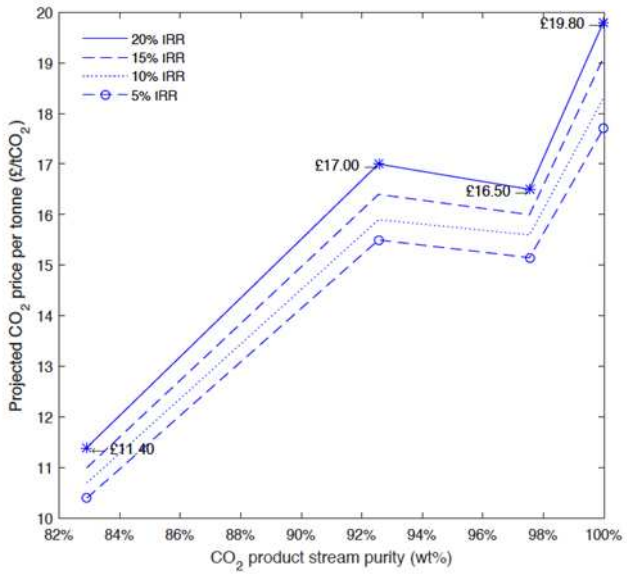

Figure 25. Graph showing the CO_2 price per tonne sold if marketed assuming a minimum rate of return on investment of 20%, 15%, 10% and 5% on the CO_2CPU as a function of CO_2 stream purity.

CO_2 Compression and Purification Units

Certain considerations must be taken into account however in terms of the product purity. A large presence of non-condensable gases can reduce storage capacity and also requires larger pipeline diameters for an equivalent amount of pure CO_2 at a given pressure. Typically it is recommended to have a purity level for CO_2 of 96% (de Visser et al., 2008). Nevertheless, if a combination of cheaper, low purity sources of CO_2 were mixed with higher purity sources of CO_2 in a transport network a final trunk line with a CO_2 stream composition suitable for injection could be achieved. In order to describe this kind of system we have taken a UK based case study with 10 gas CCGT plants, 10 coal fired plants and one steel industrial plant set up by Prada et al. (2011). Each CCGT plant was assumed to adopt amine-based post combustion capture while the coal plant and steel plant adopt oxy-combustion capture,

choosing from one of the oxy-combustion CO_2CPU models described. This scenario was formulated into a bi-objective optimization problem in GAMS, looking at the trade-offs between optimizing for lowest cost and highest purity. Binary variables of values 0 and 1 were used to represent the choice of CO_2CPU. Figure 26 shows the Pareto front for the competing objective functions: minimum cost and maximum purity assuming a lower bound for CO_2 purity at the trunk line of 96 wt.%. The results in figure 26 show the average capital and operational costs per tonne of CO_2 captured for the CO_2CPU applied to both post combustion and oxy-combustion capture. The difference between the capital cost for a minimum purity system and the maximum purity system per tonne of CO_2 capture is 45%. Applying the same assumptions as earlier for the CO_2 price, this difference represents a 17% increase in CO_2 price.

Shared Capture Plant Infrastructure

With the objective of further reducing the costs of oxy-combustion capture we have studied the financial benefits of having a shared CO_2 compression and purification unit with a throughput of 20 Mt CO_2/year (equivalent to the output of a large power plant such as Drax) as opposed to having four CO_2CPUs each with a throughput of 5Mt/year.

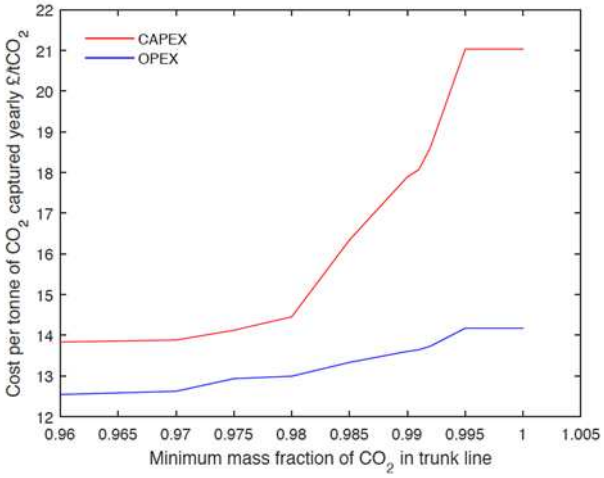

Figure 26. Graph showing the network capture system CAPEX and OPEX per tonne of CO_2 captured yearly as a function of minimum trunk line purity – optimization problem Pareto front.

In this study we do not include transport costs, however these are deemed to be significantly lower than capture costs: onshore pipelines are 25-30 times less cost intensive per tonne of CO_2 than the cost of capturing (Prada et al., 2011). The results of this study show that having one large 20Mt CO_2/year plant reduces the total capital expenditure by 16% and the yearly operating expenses by 4% compared to having four 5Mt CO_2/year units. Hence, we can conclude that adopting shared CO_2 capture infrastructure helps reduce the investment risk of CCS.

7. WP5 – CO_2 IMPURITY IMPACTS AND RISK ANALAYSIS

To fulfil the objectives of the CO_2QUEST global assessment, INERIS proposed a tool to estimate the different effects (or impacts) of various impurities in a CO_2 stream along the entire CCS chain. After a review of risk analyses for CCS performed by INERIS or by other authors[1] - completed by the expertise of CO_2QUEST partners, we identified and divided all relevant effects for impurities into three categories. i) Physical effects which have consequences on the CCS chain (e.g. reduced capacity or increased costs) without preventing its "normal" function, contrary to the other two categories that refer to CO_2 leakage, therefore an "altered" function: ii) Chemical effects may increase the probability of leakage (e.g. by pipe corrosion or by degradation of well cement). iii) Toxic/ecotoxic effects may increase the severity of any consequences arising from such a leak (e.g. if an aquifer is contaminated). Table 5 gives an overview of the 6 indicators that were finally selected (column 2). It may be observed that CO_2 stream density has an effect on transportation and storage.

[1] Mainly Farret et al., 2011[a], 2011b; Birkholtzer et al., 2009; Condor et al., 2010; Oldenburg, 2006; Savage et al., 2004; Dodds et al., 2011, Wilday et al., 2011, Mohitpour et al., 2011. Numerous other publications were also considered, either related to methodologies for risk assessment or for the description of mechanisms and their modelling.

Table 5. List of all selected indicators and the related effects

Types of effects	Selected indicators	Associated Effects	Final Impacting Phenomenon
Physical effects	CO_2 stream density	Storage volume	Reduced storage capacity
		Compression work and pipe strength	Increased energy and cost
	Interfacial tension	Storage volume	Increased storage capacity
Chemical effects	Corrosiveness	Steel pipe corrosion	Increased probability of a sudden leakage of gas at surface
	Acidity of the stream	Cement (well) porosity and integrity (leakage pathway)	Increased probability of emanation of gas at surface + contamination of aquifer
		Caprock porosity and integrity (leakage pathway)	Increased probability of emanation of gas at surface + contamination of aquifer
Tox/excotox effects	Toxic effects	Acute toxic effect	Increased severity in case of a sudden leakage of gas at surface
		Chronic toxic effect (e.g. drinking water)	Increased severity in case of contamination of an aquifer
	Ecotoxic and long-term effects	Chronic ecotoxic effect (e.g. aquifer or near-surface)	Increased severity in case of contamination of an aquifer or emanation of gas at surface

In order to perform a global assessment a semi-quantitative approach was chosen which is very common in risk analysis and is especially recommended when there is a need to compare a large range of phenomena. For each selected indicator a scoring scale ranging from 0 to 4 was proposed. For each impurity a score of 4 on each indicator is associated with an un-acceptable level of risk or consequence (or un-acceptable effect), defined by threshold values from regulation or from literature. The lower scores are then deduced, either with

linear scales (e.g. CO_2 stream density) or logarithmic scales (e.g. toxic effects). Essentially, level 0 is dedicated to absence of effect or negligible effect e.g. when the impurity concentration is below the level of detection.

The result for a whole CO_2 stream is the sum of the results for individual impurities. The 6 indicators are then displayed (see examples on figure 27 for two different CO_2 streams, as identified in Task 1 of the project). The final interpretation of the results for different capture processes is presently being performed. These 6 scores can also be summed up in order to give a global "impact index" which can in turn be combined with other social or economic criteria e.g. in a cost-benefit analysis. If necessary the requirements from such a global analysis may induce us to refine the choice of relevant indicators and scoring scales.

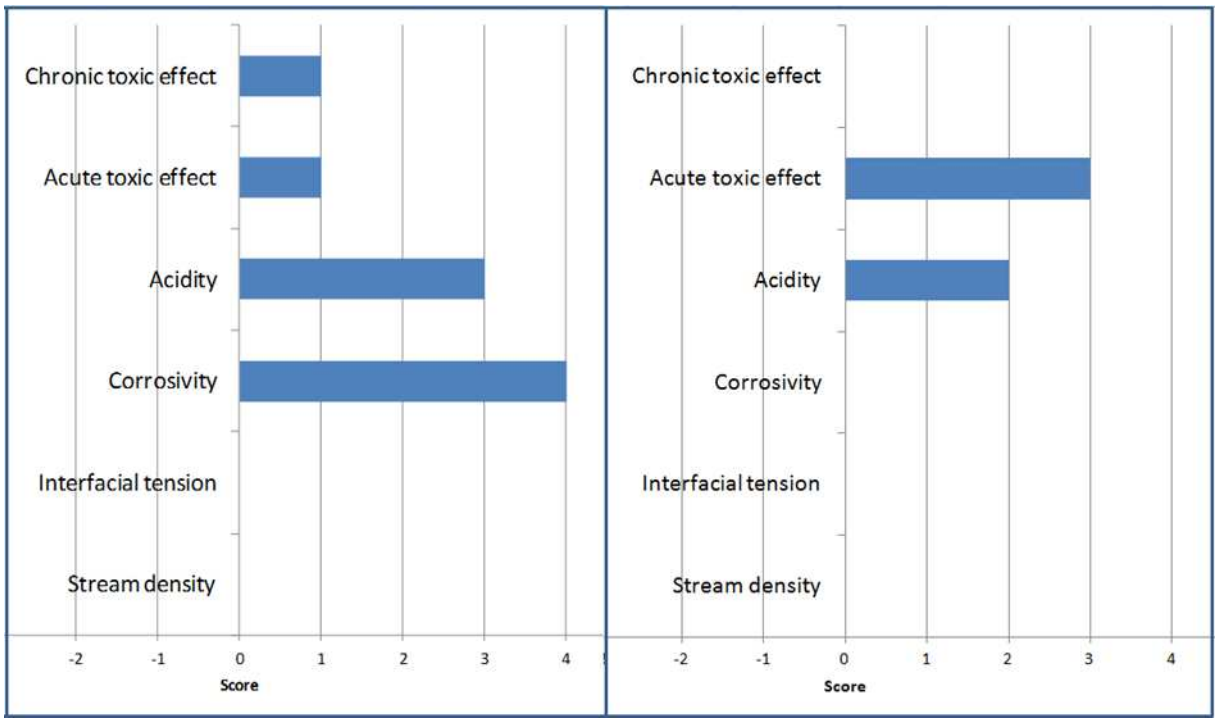

Figure 27. Display of scores for the 6 indicators for a CO_2 stream (left: a hypothetical post-combustion stream, global impact index = 9; right: a hypothetical high-purity CO_2 after pre-combustion, global impact index = 5).

8. CONCLUSIONS

Based on a comprehensive realistic-scale experimental test programme complemented with state-of-the-art mathematical modelling, the CO_2QUEST project has conducted a techno-economic assessment of CO_2 purity captured from fossil fuel power plants and industrial emission sources on its transport and storage. WP1 provided a cornerstone to the project in two main ways. First, a literature review was conducted to establish the range and level of impurities present in streams arising from the power sector and industrial CO_2 capture technologies. A cost-benefit analysis to assess the effect of CO_2 capture scenario selection on overall process costs and the CO_2 product purity was also performed. Secondly, in WP1 the development of methods and Equations of State (EoS) capable of predicting the phase equilibria, thermodynamic and transport properties of CO_2 mixtures under the wide range of fluid conditions likely to be encountered in the CCS chain was undertaken. Also in this WP EoS development was supported by numerous experiments undertaken to establish the thermophysical properties of CO_2 mixtures, including tertiary and quaternary mixtures, at the typical pressures and temperatures in CCS processes.

The focus of WP2 was on the fluid flow of CO_2 mixtures during "normal" CCS operations and during accidental high pressure releases of CO_2 following pipeline rupture in brittle or ductile fracture modes. At the same time, the impact of CO_2 impurities on the compression power requirements using various CO_2 compression strategies was investigated via the application of EoS. Additionally, the EoS have been coupled to a CFD code to simulate steady-state fluid flow within pipeline networks.

In order to provide understanding of the types of phenomenon that can occur during a high pressure CO_2 release and to provide validation data for the associated CFD simulations, CO_2 mixture experimental releases at various scales have been performed. Medium-scale controlled release experiments of CO_2 mixtures have been conducted in order to establish a better understanding of the influence of impurities on both the flow inside the pipe and on the external dispersion. Large-scale releases with pure and impure CO_2 were also performed using a purpose built and highly instrumented pipeline in Dalian, China, including on full bore releases. Also in WP2, CFD models have been developed and used to simulate impure CO_2 releases following puncture or rupture of a CO_2 pipeline. The models have incorporated EoS in order to fully account for the phase-equilibrium impacts induced by the presence of

impurities and in turn validated by comparing the results to those from the dispersion experiments conducted during the project. Investigations of three different steel materials for CCS pipelines have also been conducted to establish their response to impurities such as H_2S on corrosion as well as brittle and ductile fracture behaviour. The latter involved the development of the state-of-the-art fluid/structure interaction fracture models ultimately enabling the selection of pipeline materials properties required in order to resist long running catastrophic fractures.

WP3 was devoted to developing the understanding of the impact of impurities in the subsurface during geological storage of CO_2. To this end experiments were conducted to investigate the effect of impure CO_2 injection into the subsurface. Shallow aquifer CO_2 /impurities injection experiments conducted by INERIS in France have concluded that there is no significant impact of CO_2 impurities on aquifer contamination.

Meanwhile, the deep well CO_2 injection test experiments performed in Heletz, Israel have helped to define standard operating procedures for CO_2 injection. The geochemical impact of impure CO_2 on storage reservoir integrity in a deep saline aquifer has also been studied through modelling. A radially 2D model was constructed to simulate the relevant reactive transport models focussing on the impact of SO_2 on the brine-rock system in sandstone, showing the acidic and reactive properties of this impurity.

WP4 focussed on full-chain techno-economic analyses of CCS networks, including detailed process system simulations of different options for CO_2 purification from oxyfuel combustion and post-combustion capture technologies. The different product purities for the different CO_2 capture technologies were taken into consideration in CO_2 transport network modelling via the blending of CO_2 streams to achieve a final trunk line with a CO_2 stream of composition suitable for subsurface injection. Finally, the optimised overall CAPEX and OPEX of the full chain system was derived for the anticipated ranges of CO_2 purity for the different sources. WP5 analysed the downstream impacts of CO_2 impurities on pipeline transport and geological storage by classifying impurity impacts into physical, chemical and toxic and by developing a point scoring mechanism to describe their severity.

In conclusion, the CO_2QUEST project has provided the fundamentally important knowledge and tools needed to define the CO_2 impurity tolerance levels, mixing protocols and control

measures for pipeline networks and storage infrastructure, thus contributing to the development of relevant standards for the safe design and economic operation of CCS.

9. Acknowledgments

The research leading to the results contained in this paper received funding from the European Commission 7th Framework Programme FP7-ENERGY-2012-1 under grant number 309102. The paper reflects only the authors' views and the European Commission is not liable for any use that may be made of the information contained therein. The work by CanmetEnergy outlined in section 3.3 was supported by PERD (Program of Energy Research and Development) and the Clean Energy Fund. The authors gratefully acknowledge the support provided by these programs.

10. References

Ahmad, M., Gernert, J., & Wilbers, E., 2014. Effect of impurities in captured CO_2 on liquid–vapor equilibrium. Fluid Phase Equilibr. 363, 149–155.

Birkholzer, J.T., Zhou, Q., Tsang, C.F., 2009. Large-scale impact of CO_2 storage in deep saline aquifers: a sensitivity study on the pressure response in stratified systems. Int. J. Greenhouse Gas Control 3(2), 181–194.

Brown, S., Mahgerefteh, H., Martynov, S., Sundara, V., Mac Dowell, N., 2015. A multi-source flow model for CCS pipeline transportation networks. Int. J. Greenh. Gas Control 43, 108–114.

Brown S., Mahgerefteh, H., Martynov, S., Sundara, V., Mac Dowell, N. 2015. A multi-source flow model for CCS pipeline transportation networks. Int. J. Greenhouse Gas Control 43, 108–14.

Chapoy, A., Nazeri, M., Kapateh, M., Burgass, R., Coquelet, C., & Tohidi, B., 2013. Effect of impurities on thermophysical properties and phase behaviour of a CO_2-rich system in CCS. Int. J. Greenh. Gas Control 19, 92–100.

Chickos, J.S., 2005. Heat of sublimation data. In NIST chemistry Webbook; Linstrom, P. Mallard, W.G.; NIST Standard Reference Database Number 69; National Institute of Standards and Technology: Gaithersburg, MD, June 2005; Toluene.

CO_2PipeHaz, 2009. Quantitative failure consequence hazard assessment for next generation CO_2 pipelines: The missing link. Accessed 11/11/14; [CO_2PipeHaz Project Website]. Available from: http://www.co2pipehaz.eu/.

CO_2QUEST, 2013. Impact of the Quality of CO_2 on Storage and Transport, CO_2QUEST Project Website. http://www.co2quest.eu/ (accessed: 01.07.14).

Cole, I.S., Corrigan, P., Sim, S., Birbilis, N., 2011. Corrosion of pipelines used for CO_2 transport in CCS: is it a real problem? Int. J. Greenh. Gas Control 5, 749–756.

Condor, J., Unatrakarn, D., Wilson, M. Asghari, K., 2011. A Comparative Analysis of Risk Assessment Methodologies for the Geologic Storage of Carbon Dioxide. Energy Procedia 4, 4036-4043.

Davis, J.A., Rodewald, N., Kurata, F., 1962. Solid-liquid-vapor phase behavior of the methane-carbon dioxide system. AIChE Journal 8 (4), 537–539.

de Visser, E., Hendriks, C., Barrio, M., Mona, J., Mølnvik, M.J., de Koeijer, G. Liljemark, S., Le Gallo, Y., 2008. Dynamic CO2 quality recommendations. Int. J. Greenhouse Gas Control 2(4), 478–484.

Döbereiner, S.M. Thibaux P., 2013. Analysis of slant fracture in battelle drop weight tear tests. Proceedings of the 6th International Pipeline Technology Conference, Ostend, Belgium.

Dodds, K., Watson M., Wright I., 2011. Evaluation of risk assessment methodologies using the In Salah CO_2 storage project as a case history. Energy Procedia 4, 4162–4169.

Duan, Z., Mao, S., 2006. A thermodynamic model for calculating methane solubility, density and gas phase composition of methane-bearing aqueous fluids from 273 to 523K and from 1 to 2000bar. Geochim. Cosmochim. Ac. 70(13), 3369–3386.

Duan, Z., Sun, R., Liu, R., Zhu. C., 2007. An accurate thermodynamic model for the calculation of H_2S solubility in pure water and brines. Energ. Fuel 21(4), 2056–2065.

Edlmann, K., Niemi, A., Bensabat, J., Haszeldine, R.S., McDermott, C.I., 2016. Mineralogical properties of the caprock and reservoir sandstone of the Heletz field scale experimental CO_2 injection site, Israel; and their initial sensitivity to CO_2 injection. Int. J. Greenh. Gas Control. in press.

Fagerlund, F., Niemi, A., 2007. A partially coupled fraction-by-fraction modelling approach to the subsurface migration of gasoline spills. J. Contam. Hydrol. 89, 174–198.

Fagerlund, F., Niemi, A., Bensabat, J., Shtivelman, V., 2013. Design of a two-well field test to determine in situ residual and dissolution trapping of CO_2 applied to the Heletz CO_2 injection site. Int. J. Greenhouse Gas Control 19, 642–651.

Fandiño, O., Trusler, J.P.M., Vega-Maza, D., 2015. Phase behavior of (CO_2 + H_2) and (CO_2 + N_2) at temperatures between (218.15 and 303.15) K at pressures up to 15 MPa. Int. J. Greenh. Gas Control 36, 78–92.

Farret, R., Manceau, J-C., Le Gallo, Y., Neuville, N., 2011a. Note de synthèse Tâche 2.2: Identification de scénarios de risques de référence pour un complexe de stockage de CO_2, Convention n° 1094C0003 Ademe-GEOGREEN.

Farret, R., André, L., Brosse, E., Broutin, P., Chopin, F., Gombert, P., Jallais, S., Saysset, S., 2012. Substances Annexes au CO_2 pour un Stockage Souterrain (SACSS) - Rapport du Groupe de Travail du Club CO_2, réf. INERIS-DRS-12-127545-07346A Farret et al, SACCS.

HYSYS, 2014. Documentation: Aspen HYSYS Simulation basis. AspenTech, USA.

Jäger, A., Span, R., 2012. Equation of State for Solid Carbon Dioxide Based on the Gibbs Free Energy. J. Chem. Eng. Data**,** 57 (2), 590–597.

Jamois, D., Proust, C., Hebrard, J., 2014. Hardware and instrumentation to investigate massive spills of dense phase CO_2. Chem. Eng. Trans. 36, 601–606.

Kunz, O., Klimeck, R., Wagner, W.,Jaeschke, M., 2007. The GERG-2004 Wide-Range Equation of State for Natural Gases and Other Mixtures, GERG Technical Monograph 15, Fortschr.-Ber. VDI, Reihe 6, Nr. 557, VDI Verlag, Düsseldorf.

Mahgerefteh, H., Brown, S., 2011. Influence of Line Pressure and Temperature on Fracture Propagation Behaviour in CO_2 Pipelines, Rio Pipeline Conference and Exposition, Rio de Janeiro, Brazil, 20th-22nd September.

Mahgerefteh, H., Oke, A.O., Rykov, Y., 2006. Efficient numerical solution for highly transient flows. Chem. Eng. Sci. 61(15), 5049–5056.

Makino, H., Inoue, T., Endo, S., Kubo, T., Matsumoto, T., 2004. Simulation method for shear fracture propagation in natural gas transmission pipelines. Int. J. Offshore Polar Engineering 14, 60–68.

Martynov, S. Brown, S., 2014. CO_2QUEST Internal Report: A Report Describing the Optimum CO_2 Compression Strategy. Deliverable 2.2, University College London, UK.

Martynov, S., Mac Dowell, N., Brown, S., Mahgerefteh, H., 2015. Assessment of Integral Thermo-Hydraulic Models for Pipeline Transportation of Dense-Phase and Supercritical CO_2. Ind. Eng. Chem. Res. 54, 8587–8599.

Martynov, S., Brown, S., Mahgerefteh, H., Sundra, V., Chen, S., Zhang, Y., 2013. Modelling three-phase releases of carbon dioxide from high-pressure pipelines. Process Saf. Environ. 92(1), 36–46.

Mohitpour, M., Seevam, P., Botros, K.K., Rothwell, B., Ennis, C., 2011. Pipeline transportation of carbon dioxide containing impurities, ASME Press, New York, NY, USA.

Moore, J.J., Allison, T., Lerche, A., Pacheco, J., and Delgado, H. Development of Advanced Centrifugal Compressors and Pumps for Carbon Capture and Sequestration Applications. in The Fortieth Turbomachinery Symposium 2011, Houston, Texas 107–120.

Niemi, A. Bensabat, J, Shtivelman, V, Edlmann, K, Gouze, P., Luquot, L., Hingerl,F, Benson, S.M., Pezard, P.A, Rasmusson, K., Liang,T., Fagerlund, F., Gendler, M., Goldberg,I, Tatomir,A., Lange, T., Sauter, M., and Freifeld, B. (2016a) Heletz experimental site overview, characterization and data analysis for CO_2 injection and geological storage. Int. J. Greenhouse Gas Control, in press.

Niemi, A., Gouze, P., Bensabat, J., 2016b. Characterization of formation properties for geological storage of CO_2 - Experiences from the Heletz CO_2 injection site and other example sites from the EU FP7 project MUSTANG. Int. J. Greenhouse Gas Control, in press.

Oldenburg, C.M., 2008. Screening and Ranking Framework for geologic CO_2 storage site selection on the basis of health, safety and environmental risk. Environ. Geol. 54, 1687–1694.

Peng, D., Robinson, D.B., 1970. A new two-constant equation of state. 4th International Heat Transfer Conference, Paris, Heat Transfer 1970, volume VI, paper B.7.b.

Porter, R.T.J., Fairweather, M., Kolster, C., Mac Dowell, N., Shah, N., Woolley, R., (in prep.). CCS cost reduction potential through lower CO_2 purity levels. Int. J. Greenh. Gas Control, submitted.

Porter, R.T.J., Fairweather, M., Pourkashanian, M., Woolley, R.M., 2015. The range and level of impurities in CO_2 streams from different carbon capture sources. Int. J. Greenh. Gas Control 36, 161–174.

Posch, S., Haider, M., 2012. Optimization of CO_2 compression and purification units (CO_2CPU) for CCS power plants. Fuel 101, 254–263.

Prada, P., Konda, M., Shah, N., 2011. Development of an Integrated CO_2 Capture, transportation and Storage Infrastructure for the UK and North Sea using an Optimisation Framework. AIChe Annual Meeting, Minneapolis, October 17th 2011.

Pruess, K., 2004. The TOUGH codes - a family of simulation tools for multiphase flow and transport processes in permeable media. Vadose Zone Journal, 3(3), 738–746.

Pruess, K., Spycher, N., 2007. ECO2N – A fluid property module for the TOUGH2 code for studies of CO_2 storage in saline aquifers. Energ. Convers. Manage. 48(6), 1761–1767.

Rasmusson, K., Rasmusson, M., Fagerlund, F., Bensabat, J., Tsang, Y., Niemi, A., 2014. Analysis of alternative push-pull-test-designs for determining in-situ residual trapping of carbon dioxide. Int. J. Greenhouse Gas Control 27, 155–168.

Rebscher, D., Wolf, J. L., Jung, B., Bensabat, J., Segev, R., and Niemi, A. P., 2014. Effects of impurities in CO_2 spreading model development for field experiments in the framework of the CO_2QUEST Project, AGU Fall Meeting, Vol.1, H21A-0708, 2014.

Savage, D., Maul, P.R., Benbow, S., Walke, R.C., 2004. A generic FEP database for the assessment of long-term performance and safety of the geological storage of CO_2. Quintessa Report QRS-1060A-1.

Serpa, J., Morbee, J., Tzimas, E., 2011. Technical and Economic Characteristics of a CO_2 Transmission Pipeline Infrastructure, in, Joint Research Centre Institute for Energy, Petten.

Sim, S., Cole, I.S., Bocher, F., Corrigan, P., Gamage, R.P., Ukwattage, N., Birbilis, N., 2013. Investigating the effect of salt and acid impurities in supercritical CO_2 as relevant to the corrosion of carbon capture and storage pipelines. Int. J. Greenh. Gas Control 17, 534–541.

Span, R., Eckermann, T., Herrig, S., Hielscher, S., Jäger, A., Thol, M., 2015. TREND. Thermodynamic Reference and Engineering Data 2.0.1, Lehrstuhl fuer thermodynamik, Ruhr-Universitaet Bochum.

Talemi, H.R., Steinhoff, M., Cooreman S., Van den Abeele, F., Verleysen, P., 2016a. Effects of high strain rates on ductile slant fracture behaviour of pipeline steel: experiments and modelling. Proceedings of the 11th International Pipeline Conference (IPC2016), Calgary, Alberta, Canada.

Talemi, H.R., Cooreman S., Van Hoecke, D., 2016b. Finite element simulation of dynamic brittle fracture in pipeline steel: A XFEM-based cohesive zone approach. Proc. Inst. Mech. Eng., Part L.

Talemi, H.R., 2016. Numerical simulation of dynamic brittle fracture of pipeline steel subjected to DWTT using XFEM-based cohesive segment technique, Frattura ed Integritá Strutturale, accepted for publication.

Wang, J., Ryan, D., Anthony, E.J., Wigston, A., Basava-Reddi, L., Wildgust, N., 2012.The effect of impurities in oxyfuel flue gas on CO_2 storage capacity. Int. J. Greenh. Gas Control 11, 158–162.

Wareing, C.J., Woolley, R.M., Fairweather, M., Falle, S.A.E.G., 2013. A composite equation of state for the modeling of sonic carbon dioxide jets in carbon capture and storage Scenarios, AIChE J. 59, 3928–3942.

Wetenhall, B., Race, J.M., Downie, M.J., 2014. The effect of CO_2 purity on the development of pipeline networks for carbon capture and storage schemes. Int. J. Greenh. Gas Control 30, 197–211.

Wilday, J., Paltrinieri, N., Farret, R., Hebrard, J., Breedveld, L., 2011. Addressing emerging risks using carbon capture and storage as an example. Process Safety and Environmental Protection 89, 463–471.

Witkowski, A., Majkut, M., 2012. The Impact of CO_2 Compression Systems on the Compressor Power Required for a Pulverized Coal-fired Power Plant in Post-combustion Carbon Dioxide Sequestration. Archive Mech. Eng. 59(3), 343–360.

Wolf, J.L., Niemi, A., Bensabat, J., Rebscher, D. (in prep.). Benefits and restrictions of 2D reactive transport simulations of impurities co-injected with CO_2 in a saline aquifer, Int. J. Greenhouse Gas Control, in preparation.

Woolley, R.M., Fairweather, M., Wareing, C.J., Proust, C., Hebrard, J. Jamois, D., Narasimhamurthy, V.D., Storvik, I.E., Skjold, T., Falle, S.A.E.G., Brown, S., Mahgerefteh, H., Martynov, S., Gant, S.E., Tsangaris, D.M., Economou, I.G., Boulougouris, G.C., Diamantonis, N.I., 2014. An integrated, multi-scale modelling approach for the simulation of multiphase dispersion from accidental CO_2 pipeline releases in realistic terrain. Int. J. Greenh. Gas Control 27, 221–238.

Woolley, R.M., Fairweather, M., Wareing, C.J., Falle, S.A.E.G., Proust, C., Hebrard, J., Jamois, D., 2013. Experimental measurement and Reynolds-averaged Navier–Stokes modelling of the near-field structure of multi-phase CO_2 jet releases, Int. J. Greenhouse Gas Control 18, 139–149.

Woolley, R.M., Fairweather, M., Wareing, C.J., Proust, C., Hebrard, J., Jamois, D., Narasimhamurthy, V.D., Storvik, I.E., Skjold, T., Falle, S.A.E.G., Brown, S., Mahgerefteh, H., Martynov, S., Gant, S.E., Tsangaris, D.M., Economou, I.G., Boulougouris, G.C., Diamantonis, N.I., 2014. An integrated, multi-scale modelling approach for the simulation of

multiphase dispersion from accidental CO_2 pipeline releases in realistic terrain, Int. J. Greenhouse Gas Control 27, 221–238.

Xu, T., Sonnenthal, E., Spycher, N., Zheng, L., 2014. TOUGHREACT V3.0-OMP Reference Manual: A Parallel Simulation Program for Non-Isothermal Multiphase Geochemical Reactive Transport, LBNL-DRAFT. - Lawrence Berkeley National Laboratory, University of California, Berkeley.